CHARACTERIZATION OF PVA HYDROGELS WITH REGARDS TO VASCULAR GRAFT DEVELOPMENT

A Thesis
Presented to
The Academic Faculty

by

Tarek Elshazly

In Partial Fulfillment
of the Requirements for the Degree
Masters of Science in Mechanical Engineering

Georgia Institute of Technology
May 2004

CHARACTERIZATION OF PVA HYDROGELS WITH REGARDS TO VASCULAR GRAFT DEVELOPMENT

Approved by:

Dr. David Ku, Advisor

Dr. Alexander Rachev

Dr. Raymond Vito

April 8, 2004

ACKNOWLEDGEMENTS

I am very thankful to the Georgia Institute of Technology and the associated faculty and staff for providing me with an excellent engineering education. I especially thank Dr. David Ku for his advisement in conducting the research presented in this document. I sincerely thank Dr. Alexander Rachev for the many hours he spent helping me understand complicated material and proper experimental design. I also thank the third member of my committee, Dr. Raymond Vito, who was helpful in reviewing and revising this document and improving my work. Lastly, thanks to my family and friends, whose support and companionship I could always count on.

TABLE OF CONTENTS

LIST OF TABLES

LIST OF FIGURES

SUMMARY

Three main areas of research are conducted on polyvinyl alcohol (PVA) hydrogels with the intent to validate or refute continued development of these materials as arterial substitutes. The research areas are listed below, along with a summary of their association to vascular grafts.

1. **Mechanical characterization of PVA hydrogels** – Provides a tool for graft design and analysis, which is needed to produce circumferentially and longitudinally compliance-matched grafts. The mechanical response of a graft also effects surrounding tissue, as excessive cellular proliferation (hyperplasia) is hypothesized to be highly dependent on the graft stress-strain environment.

2. **Cell adhesion to PVA hydrogels** – Demonstrates the potential to form a monolayer of endothelial cells on the inner graft surface, which is a possible strategy to mitigate the thrombogenic response.

3. **Cryo-high resolution SEM study of PVA hydrogels** – Identifies a tool to observe the polymer network of PVA hydrogels in the hydrated state, which is helpful to explain limiting material-tissue interactions incurred upon graft implantation.

CHAPTER 1

INTRODUCTION

1.1 Abstract

Synthetic vascular grafts represent a leading strategy to treat patients with dysfunctional, compromised, or injured arteries. Such treatment is immensely important, as arterial occlusive disease is a problem of epidemic proportions in our aging society. Although large and medium sized grafts are routinely used in clinical applications, these devices lack the desired efficacy and are not useful for small diameter prosthesis.

Polyvinyl alcohol (PVA) hydrogels are potential materials for vascular graft development. The properties of these materials are similar to native tissue, and can be adjusted and controlled through manufacturing techniques. Three broad aspects of appropriation for almost all biomaterial applications are addressed in this research, producing the following results:

1. Complete mechanical characterization of PVA hydrogels
2. Demonstration of cell adhesion to PVA hydrogel surfaces
3. Use of a new microscopic technique to view the polymer network of PVA hydrogels

These areas of research are relevant to a vascular graft application, and increase the knowledge of this potentially revolutionary biomaterial.

1.2 Synthetic vascular grafts

Vascular grafts are devices intended to replace compromised arteries throughout the body. Due to the complex and poorly understood physiologic responses to a vascular implant, only medium to large diameter vascular grafts are currently produced. Grafts of less than 6-mm in diameter have proved elusive to researchers, displaying uncontrollable responsive phenomena such as thrombogenisis, intimal hyperplasia, and incomplete healing [1,2]. Although graft research and development is in its fourth decade, disagreements on fundamental design concepts persist. A lack of a consensus in the field exists with respect to graft material, desirable characteristics, and methods of healing induction [1]. An understanding of the current milestones and limitations of large diameter grafting gives insight into what is needed for the production of patent, small diameter grafts.

The problems preventing small diameter grafting also arise in larger diameter grafts, and are the limiting factors that determine graft lifespan. Improved control of the physiologic responses following implantation will increase the efficacy of existing grafts and make small diameter grafting feasible. The following obstacles hinder the development of all synthetic vascular grafting:

1. Blood-material interactions and the instigation of the thrombogenic response [3].

2. Excessive cellular proliferation occurring within and around the graft, specifically the occurrence of intimal hyperplasia, which has been correlated to regions of disturbed flow or low shear stress [4].

3. Compliance of the graft in response to fluctuations in blood pressure and the need for a compliance match between the graft and the adjacent vasculature [5].

4. Appropriate mechanical properties of the graft throughout the physiologic stress range.

Despite the complexity associated with vascular graft development, numerous possible solutions have been proposed. The most important factor is clearly the selection of the graft material [1]. Many synthetic materials with the appropriate range of mechanical properties have been identified for vascular graft application. The next step is to determine which material can be processed and prepared to sufficiently overcome the aforementioned obstacles. The following material characteristics, processing parameters and preparation techniques influence graft patency:

1. Inherent material compatibility with respect to blood-material interactions and instigation of the immune response to an implanted device.

2. Porosity of the material, which effects cellular and molecular adhesion and diffusion through the graft [6,7].

3. The processing of a material to control the mechanical properties of the graft. For example, the extent of physical crosslinking induced between monomers of a hydrogel to control to the burst strength of a tubular sample.

4. *In vitro* endothelialization of the luminal graft surface prior to implantation as a means to suppress blood-material interactions and reduce the thrombogenic response [8,9].

5. Peptide and protein coatings on the graft surface to promote *in vivo* and *in vitro* endothelialization and graft healing following implantation [10,11,12].

6. The surface texture of the graft as a means to control cellular and protein adhesion.

7. Interrupted anastomotic suturing to promote a compliance match specifically at the graft suture site [5].

The experimental approaches listed above are by no means exhaustive, as the constantly growing body of literature on vascular grafts has expanded to include a variety of techniques. However, these factors are amongst the most heavily researched, and hold great promise for the future of synthetic vascular grafting. A closer look at the status of existing grafts indicates the obstacles of development of a patent, small diameter vascular graft.

Large and medium diameter synthetic vascular grafts

Large diameter grafting is consistently improving and is commonly used in a clinical setting to replace compromised vasculature. Compared to small diameter grafts, medium to large diameter grafts have a much higher margin for error in terms of implantation demands. Larger grafts can maintain patency despite basal thrombogenic, hyperplasic, and immune activation due to the sufficient volumetric blood flow and large cross sectional area. With small diameter implants, the blood-material interactions are severe enough to impede the luminal flow and lead to dangerous emboli formation.

Methods of improving biocompatibility, such as heparinization, are commonly utilized in such larger grafting procedures. Polyethylene terephthalate (Dacron) and expanded polytetrafluoroethylene (ePTFE) are the standard materials used in large vessel replacement, with Dacron being used in approximately 80% of synthetic grafting procedures. Both of these materials demonstrate successful clinical application in 6-mm internal diameter prosthesis with regards to prevention of activation of procoagulatory blood components, necessary mechanical strength, immune acceptance, suturability, and acceptable patency rates [13]. However, attempts at smaller diameter grafting (internal

diameter less than 6-mm) with either material results in acute thrombus formation [14, 15] and chronic anastomotic hyperplasia [16, 17,18] to a clinically unacceptable extent.

Dacron was first commercially available in 1951 and was used in clothing, curtains, belts, fire hoses, and filled products. This polyester fiber is a registered trademark of Dupont and has since been used to develop numerous products. Until the introduction of PTFE in the 1970's, Dacron was considered the leading candidate material for the development of synthetic vascular grafts.

Dacron grafts are currently produced with three basic formations, with each corresponding to a particular philosophy on dealing with the physiological events unfolding in the graft [1]. Woven, knitted, and high porosity velour graft designs have all been used in a clinical setting.

Woven grafts contain a low level of porosity, which corresponds to excellent graft strength and mechanical patency. The porosity of these grafts only allows for minimal neointimal formation when implanted in humans, usually after a period of about 10 years [19,20]. However, this growth is far from the desirable confluent endothelial cell (EC) monolayer, and would not prevent blood-material interactions as needed in a small diameter implant. The level of implant healing can be estimated by the ingrowth of microvasculature into the graft, which is also minimized or excluded in the low porosity setting of woven grafts [21].

Knitted Dacron presents a higher level of porosity with an associated increase in general adherence to the graft [22]. Endothelialization and microvasculature formation are accelerated in the knitted structure, contributing to improved prosthesis blood compatibility and healing. However, a fibrin matrix containing white blood cells,

erythrocytes, and platelets also arises shortly after implantation [22]. Studies have shown that this inner fiber capsule can reach a thickness of up to 500 μm within 5 weeks following human implantation, with no indication of reaching growth equilibrium. Such levels of adherence and fibrous accumulation would lead to quick occlusion in small diameter applications [23].

High porosity Dacron velour is a graft design comprised of various porosity regions. In this formation, a knitted graft is essentially covered with a finer and more evenly distributed porous structure [24]. The finer material is applied as an external and internal cover to the graft, and is intended to improve healing of the prosthesis. The velour grafts have shown similar clinical results as the knitted Dacron, and are clearly not suited for small diameter grafts due to prolonged and intense platelet activation [25]. Simply reducing the dimensions of the current Dacron products does not adequately meet the requirements of a small diameter graft.

Expanded polytetrafluoroethylene (ePTFE) is the second most common material for current grafting applications. Grafting with ePTFE results in products with a low level of immune activity [26], sufficient burst and tensile strengths, and easy incorporation into the vasculature [27]. ePTFE grafts are superior to Dacron grafts with respect to improved patency rates, decreased thrombogenic reactions, and resistance to infection. Despite these desirable characteristics, small diameter grafting with ePTFE has yielded no viable products [28]. Attempts to implant strategically engineered small diameter ePTFE grafts could not prevent thrombogenic formation and eventually graft occlusion in numerous animal studies [1].

Small diameter synthetic vascular grafts

The development of small diameter vascular grafts is a unique problem of scale. Grafts of 6-mm or greater internal diameter remain patent and are clinically acceptable, while otherwise identical grafts of smaller diameter fail due to thrombus formation [14, 15] or flow-restrictive intimal hyperplasia [16,17,18]. Although the technology and understanding of the aforementioned large diameter grafts is at a level where implants are routinely performed with successful results, the field has not produced a patent, small diameter graft. A small amount of thrombogenic activity can be tolerated in large vessels, but can have dire consequences in a small diameter graft. With current materials and techniques, platelet activation in a synthetic vascular graft is unavoidable to some extent, and often leads to dangerous circulatory inhibition in small diameter grafts. Clearly, a new approach to these problems is needed to produce a synthetic small diameter graft.

Numerous design parameters have been identified as highly influential for graft patency. Material porosity, endothelialization, compliance matching, material selection, material processing, and animal modeling are all current foci of vascular graft development, as described in the subsequent sections.

Issues in vascular graft design

Porosity

Various material parameters have been identified as possible methods to control the physiologic response to small diameter vascular grafts. Porosity can be induced in virtually any biomaterial, and is highly influential in controlling cell migration throughout a structure [28,29]. Studies involving PTFE grafts have shown that cell migration and resulting graft healing are highly dependent on material porosity [30]. In

relation to small diameter vascular grafts, the use of porosity induction has both positive and negative consequences [31]. The transmigration of smooth muscle cells (SMC) from the interstitial tissue into the graft and the endothelialization of the blood-contacting surface are hypothesized to improve the compliance and compatibility of the material, respectively. In native tissue, the compliance of an artery, which is a mechanical response to the stresses imposed by the blood flow, effects SMC proliferation rates within the media and EC alignment and proliferation in the intima.

Despite this apparent need for SMC inclusion, an effective porous configuration has yet to be engineered. As SMC and EC integration into the graft proceeds following implantation, neointimal hyperplasia is observed in porous Dacron and ePTFE grafts and is expected in all similar materials [1, 32]. The influx of cells into the internal layer of the graft has spatial limitations, which will compromise the lumen of the implant and lead to occlusion. In addition, porosity has been shown to increase the adhesion of macrophages, fibrinogen, and other molecules that form an increasingly adverse microenvironment throughout the graft [32]. Porosity is a promising technique that must be further explored as a method of controlling cell migration and promoting various types of adhesion, with tissue engineering applications extending beyond synthetic vascular grafting.

Endothelialization

The intimal layer of a native vessel is comprised of a network of various proteins that are covered with a monolayer of EC. The endothelium is thus the contact surface between the artery and the blood tissue. Any injury to this cell layer instigates a host of blood responses, which attempt to mitigate the injury through clotting and eventual

reconstitution of the cellular component. In fact, no surface is known to placate the blood response with the efficacy of the EC monolayer.

Mimicry of the intima is a logical approach to improve the blood-material interactions involved in synthetic vascular grafting. If a biomaterial is coated with a monolayer of healthy EC, the interaction with the blood tissue will be extremely similar if not identical to normal physiologic conditions [33]. Canine studies involving polyurethane scaffolds seeded with SMC and EC have shown retention of the cell layers and graft patency for up to four weeks in carotid arteries [34]. Polyurethane grafts have also been electrostatically seeded with EC, with studies indicating enhanced neointimal development and reduced incidence of thrombosis in canine femoral arteries [35]. Instead of attempting to minimize the thrombogenic response of the blood tissue to a biomaterial, endothelialization attempts to bypass this interaction [33,36].

Numerous problems are associated with endothelialization and have prevented the use of this technique. Two main approaches are under current investigation in the field: *in vitro* cell seeding prior to implantation and recruitment of cells from the blood stream and interstitial tissue following implantation. Neither technique has provided a holistic solution for the integration of an EC monolayer with a biomaterial surface.

In vitro seeding prior to implantation introduces problems such as storage and delivery of the graft containing a living element. However, studies have shown that a freeze-drying technique can be applied to both Dacron and PTFE grafts at a state featuring the appropriate substrate coating for endothelialization [33]. These ‘ready to seed’ grafts approach the goal of ‘ready to use’ grafts, but would still require cell seeding and culturing time prior to implantation.

Cell recruitment from the host following implantation is a technique that avoids the cell storage and delivery problems, but is difficult to control in practice. The difficulty of this control is further complicated by the differential response from patient to patient and the lack of a representative animal model [37, 38]. Nevertheless, development of tissue-engineered biointeractive polymers has shown that EC recruitment is effected by internodal distances of a fibrin glue impregnated with FGF-1 and heparin in a canine model [12]. However, concurrent cell recruitment of EC and SMC is difficult to control and appropriate for a vascular graft application, with indication of high sensitivity to the FGF:heparin ratio. Other studies have effectively used protein domains to improve neointimal formation, which provide a higher level of conformational complexity than the more heavily researched peptide sequence inserts [39]. Despite the progress made in this approach, many questions remain unanswered as to the optimization and use of this technique for a therapeutic option.

Perhaps the most fundamental and impeding question regarding endothelialization is one of cell sourcing. The EC used must be derived from the patient for whom a particular graft is prepared. Any other source, animal or human, will result in immune rejection and graft failure. A few possibilities for cell sourcing have been suggested and are currently being explored, including the use of stem cells or the recently identified circulating EC. Both sources are highly questionable in terms of feasibility and efficacy, but research is underway nevertheless. Small diameter grafting, as well as the entire field of tissue engineering, is currently at standoff with the issue of cell sourcing for tissue-engineered products.

Compliance matching

The mechanical compliance of a biomaterial was first hypothesized to affect the patency of vascular grafts in 1976 [40]. Experimental verification of this theory came 11 years later, when increased blood flow impedance, disturbed turbulence, and low shear stress rates were identified as results of compliance mismatches between the native vasculature, the anastomosis, and the graft [41]. Since then, flow disturbances, particularly those that reduce the vessel shear stress, have been correlated to the occurrence of intimal hyperplasia [4]. A compliance match of a synthetic vascular graft is thus essential for patency, especially for spatially limited small diameter prostheses.

Compliance of synthetic grafts has been evaluated from both the longitudinal and the circumferential responses. Due to the importance of cross sectional area in synthetic grafts, the circumferential compliance has proved to be much more relevant when evaluating graft efficacy and is currently the parameter of interest [5]. Once again, the body of researchers working on vascular grafts has not reached a consensus, as various methods for evaluating the circumferential compliance are used. The techniques that are currently utilized include optical, x-ray, ultrasonic, and magnetic resonance imaging, with pros and cons accompanying each method. The problem with variable measurement methods is evident; data derived from different methods, and often from the same method with different interpretation, cannot be compared.

Compliance of a graft can arise from both biologic and synthetic sources. The active SMC control of the native artery diameter in response to blood pressure has been previously mentioned, and is relevant to the mechanical compliance of a synthetic graft featuring SMC adherence. However, complications arise from the uncontrollable

proliferation of SMC (and EC) which can compromise the flow through the graft lumen. Despite this difficulty, SMC seeding or recruitment is a possible method to improve circumferential compliance matching in synthetic grafts.

The inherent mechanical properties of a biomaterial are the main aspect of design that can be used to affect compliance matching between a graft, the native vasculature, and the sutured regions. Material selection for the prosthesis has been primarily focused on biocompatibility, but is now being expanded to include compliance matching. The mechanical properties of most materials can be varied through processing techniques, although the coupled effect on biocompatibility may vary from one material to another. Compliance matching from a materials standpoint would greatly benefit from a field standardization of measurement and evaluation, as an accumulation of material data would facilitate graft design.

***In vivo* and *in vitro* limitations**

The progression of all bioengineered products is hindered by the limitations imposed by both *in vitro* experimentation and animal studies. Nothing short of clinical trials on human subjects can elucidate exactly how a material or device will function following its application. Clinical trials are required by the FDA and are a part of typical product development, but usually are not conducted until the product is near full maturity. The lack of an animal model or *in vitro* experimental set up to indicate the likely human response is a major problem for the field focused on vascular graft development.

In addition to the general limitations of *in vitro* and animal studies, vascular graft research is further limited by the differential hemocomposition between humans and test

animals. The blood-material interactions in canine, porcine, baboon, and in fact all animals are different to those in humans. In particular, the dynamics of cellular ingrowth and thrombogenicity are notably different across species, which greatly reduces the significance of animal models [37, 38]. The limitations of pre-clinical trial studies to evaluate vascular graft efficacy accentuates the need for coherence of testing standards and graft characterization throughout the research community.

1.3 PVA hydrogels as a potential material

The necessary properties of a vascular graft include biocompatibility, a nonthrombogenic inner surface, physical durability, compliant properties similar to the native tissue, resistance to infection, ease of manufacturing and ease of implantation [5]. PVA hydrogels are water swollen, cross linked polymers with great potential to satisfy these identified graft demands. Previous studies and applications of PVA hydrogels have shown the materials to be biocompatible, durable, and easy to manufacture, and suggest that other graft requirements are also likely met by these materials.

The appearance and feel of PVA hydrogels are similar to native arterial tissue. PVA hydrogels have a significant range of mechanical properties based on compositional and processing parameters. This notable mechanical variance will facilitate the design of a graft with compliant properties similar to the surrounding tissue. These materials are hydrophilic and thus likely capable of protein absorption and supporting healthy cellular growth. Such biointeractive properties allow for the possibility of using EC to create a nonthrombogenic inner graft surface. PVA hydrogels have great potential as a grafting material, and are also candidates for a wide range of other biomaterial applications.

Experimental Descriptions

1.4 Mechanical characterization of PVA hydrogels

Determination of the constitutive equations for PVA hydrogels will completely mechanically characterize the materials. Assuming that PVA hydrogels manifest predominantly elastic mechanical response under loads, a strain energy function (SEF) exists from which the constitutive equations can be derived. In general, identification of the SEF requires data form three-dimensional or biaxial mechanical testing, for compressible and incompressible elastic materials, respectively.

In this study, mechanical testing of PVA hydrogels is conducted to measure the response of the materials in uniaxial tension. A strain energy approach is then used to process the results of the uniaxial tensile tests and predict a three-dimensional response of an internally pressurized thick-walled tube fabricated from a particular PVA hydrogel. Verification of the proposed SEF is achieved through comparison of the predicted and experimental pressure-diameter response of the hydrogel tube. Mechanical characterization of a potential vascular grafting material will facilitate circumferential and longitudinal compliance matching following implantation, which is a possible strategy to improve graft patency.

1.5 Feasibility study of cell adhesion to PVA hydrogels

This study is focused on rating the *in vitro* adhesion of Bovine Aortic Endothelial Cells (BAEC) to the surfaces of various PVA hydrogels. The strength of adhesion is tested with a physiologic flow loop, which is designed to impart PVA hydrogel samples with the shear stress arising in the native artery. Surface roughness is varied across PVA hydrogel samples in order to determine if micron-level topology can enhance BAEC adhesion. Cell counts and adhesive cell morphologies are used to compare samples. BAEC adhesion in this study is indicative of the potential for human endothelial cell (HEC) adhesion to PVA hydrogels. *In vitro* and *in vivo* endothelialization of the inner surface of synthetic vascular grafts are possible strategies to minimize the thrombogenic response of an implant.

1.6 cHRSEM study of PVA hydrogels

Cryo-high resolution scanning electron microscopy (cHRSEM) is a revolutionary analytical imaging tool that provides nanometer resolution without sample distortion. This technique allows for observation of a hydrogel polymer network in the hydrated, undisturbed, water-swollen state. The goal of this study is to obtain and catalog high magnification images of two PVA hydrogels using cHRSEM. Such observation increases the understanding of molecular interactions of the hydrogel with its surroundings, and can lead to improved sample preparation for various biomaterial applications. In the case of vascular graft development, the surface characteristics of the PVA hydrogel can be modified to control the interactions of the graft inner surface with the blood tissue.

1.7 List of specific aims

1. Determine the mechanical response of PVA hydrogels in uniaxial tension. Use a constitutive approach to analyze the one-dimensional response and propose a SEF for the material. Verify the accuracy of the proposed SEF by comparing the theoretical predictions and experimentally recorded data of the mechanical response of a structure under more general load conditions.

2. Determine if a PVA hydrogel can serve as a scaffold for adhesion of BAEC under physiologic flow conditions. Quantify the effect of micron-level hydrogel surface roughness on cellular adhesion.

3. Catalog cHRSEM images of the hydrated, polymeric network of two PVA hydrogels with high resolution and up to 50,000 X magnifications.

1.8 Hypothesis

1. PVA hydrogels can be considered as nonlinear, elastic, isotropic, incompressible materials. They belong to the class of materials for which the SEF is a function of only the first invariant of Green strain tensor. Therefore, the results of one-dimensional testing are sufficient to identify a SEF and fully characterize the mechanical properties of PVA hydrogels.

2. Due to the hydrophilic nature of PVA hydrogels and the results of similar cell seeding experiments, successful BAEC adhesion is expected. Furthermore, the presence of micron-level roughness on the material surface should improve the anchorage of cellular focal adhesion sites. This improvement should manifest as enhanced cellular maintenance on the PVA hydrogel surfaces featuring roughness following exposure to a physiologic flow loop.

3. The use of cHRSEM is expected to provide the resolution to observe the polymer network of both tested PVA hydrogels. It is also expected that some water is intimately incorporated into the hydrogels and that extensive polymeric networks are visible, due to the compressibility and strength of the materials, respectively.

CHAPTER 2

MATERIALS AND METHODS

2.1 Mechanical characterization of PVA hydrogels

Uniaxial tensile testing of a strip

PVA hydrogel samples (average M_w 124,000 – 186,000, provided by Aldrich Chemical Company, Inc) are prepared for the purpose of uniaxial tensile testing. The samples differ in PVA percentage and freeze/thaw cycling scheme, with six total variations. The processing and composition characteristics along with the hydrogel sample numbers are presented in Table 1.

To prepare a hydrogel sample, a PVA/H_20 mixture is formed based on the desired weight percentage (10% or 15% for this experiment). The mixture is then autoclaved on a liquid cycle with a chamber temperature of 121°C and a sterilization time of 25 minutes to form a homogeneous solution. The solution is cast into a rectangular mold at an elevated temperature (>100°C) and treated with a freeze/thaw cycling scheme. A single cycle Table 1 refers to 8 hours of freezing at –20.0°C and 4 hours of thawing at 22°C. All cycles are applied sequentially for the desired number of repetitions. Following cycling completion, the rectangular specimens are carefully cut into the traditional dog bone shape used for uniaxial extension experiments, as sketched in Figure 1. The samples are then stored in an aqueous solution at room temperature until mechanical testing (storage time is approximately 24 hours for all samples).

Uniaxial tensile testing is conducted on an EnduraTec ELF 3200 mechanical tester (provided by Bose, Inc.). A 5 lb load cell is used to apply a displacement rate-controlled (1mm/sec) tensile force to the PVA hydrogel samples. Force and displacement

data are acquired with a Wintest software program and are exported as a data file for analysis.

Uniaxial tensile testing of a ring

The previously described uniaxial extension experiments are conducted for the purpose of gathering data to identify a SEF for six variations of PVA hydrogels. Verification of the proposed SEF will require using one-dimensional data to accurately predict the mechanical response under more general loading conditions, such as the case of an internally pressurized thick-walled tube (three-dimensional deformation).

To this end, PVA hydrogel tubes are acquired from a biomaterial company. The details of the compositional and processing parameters of these samples are kept confidential in the interest of the provider [42]. Physical crosslinking of the PVA hydrogel network is induced through temperature cycling in a process similar to the previously described strip sample preparation. Ring shaped samples are cut from the tubes, with enough of each tube kept intact for subsequent tube inflation testing (Figure 2). The dimensions of the rings are recorded and the ring samples are studied in uniaxial extension. The same mechanical tester is used to apply uniaxial extension, which again summarizes the extension as force-displacement data.

Tube inflation testing

A thick-walled tube kept at constant length is inflated by applying an internal pressure. A closed loop system composed of a PVA hydrogel tubular sample, additional tubing, a pressure transducer, a flow-restriction valve, and a syringe is used to apply an internal pressure, as depicted in Figure 3. The internal pressure is created by pushing water through the closed loop with the syringe, and is measured by the pressure

transducer. Digital calipers are used to measure the external diameter of the PVA hydrogel tube at internal pressures ranging from 0 – 600 mmHg, with a 50 mmHg step. Pressure-diameter data are recorded for three PVA hydrogel tubes, which are used for verification of the proposed mechanical characterization in terms of a SEF.

2.2 Feasibility study of cell adhesion to PVA hydrogels

Hydrogel preparation

Granular PVA (average M_w 124,000 – 186,000, provided by Aldrich Chemical Company, Inc.) is prepared as a hydrogel of specific weight concentration by mixing with DI, filtered H_2O. The PVA/H_2O mixture is then autoclaved on a liquid setting with the following cycle parameters: chamber temperature 121°C, sterilization time 25 minutes. A homogeneous, clear solution is formed and stored at 100°C until it is cast.

Surface roughness induction

Nylon micromesh (27 – 250 μm squares, provided by Small Parts, Inc.) patterns are imprinted (imprinting mass of 6.8 kg) onto aluminum sheets and cut to fit the wells of 12-well polystyrene tray (well diameter of 2.54 cm). The micromesh imprints are positioned at the base of the wells. A 10 ml pipette is used to fill each well cavity with 1.5 ml of the prepared PVA/H_2O solution. The cast solution is then processed with a freeze/thaw cycling scheme (freeze at –20.0ºC for 8 hours, thaw at 22ºC for 4 hours, repeated 4 times consecutively) to induce physical crosslinking of PVA monomers and formation of the PVA hydrogel.

Cell culturing

Cryopreserved BAEC (provided by Cambrex Bio Science Walkersville, Inc.) are cultured at the 7th passage with the following media and treatment:

Media composition:

93% Dubelco's modified eagle medium (provided by Gibco)

5% Fetal bovine serum (provided by Cellgro)

1% L-glutamine (provided by Cellgro)

1% antibiotic cell support solution (provided by Sigma)

Incubator specifications:

Water jacketed insulator (provided by Forma Scientific)

Chamber temperature of 37°C

CO_2 concentration of 5%

BAEC are cultured on 75 cm^2 treated, non-pyrogenic, sterile, polystyrene flasks (provided by Corning) with an initial seeding density of 4000 cells/cm^2. After the culture reached confluence, trypsinization (Trypsin-EDTA, provided by Gibco) is performed and the cells are seeded onto the prepared PVA hydrogel samples.

Cell seeding onto PVA hydrogels

Prior to cell seeding, all PVA hydrogel samples are sterilized with a 24 hour UV exposure and coated with a layer of Type 1 purified collagen (3:1 collagen concentration, provided by Vitrogen). A seeding density of approximately 4000 cells/cm^2 is applied to the surface of each sample. All samples are then cultured for 72 hours. Following this treatment, the samples are cut in half. One half of each sample remains in static culture conditions for an additional 24 hours. The other halves are used to generate 35 mm^2 specimens for dynamic testing in the physiologic flow loop.

Physiologic flow loop

A physiologic flow loop is used to apply a shear stress of 20 dyn/cm^2 to cell seeded PVA specimens for 24 hours. The specimens are secured in a rectangular window located in the sample housing of the flow loop, as shown in Figure 4. Based on the

following equation, a flow rate of 36.5 ml/min is calculated to impart the desired shear stress on the PVA specimens.

$$Q = \frac{\tau H^2 b}{6\mu} = \frac{(20\text{dyn/cm}^2)(0.026\text{cm})^2(2.7\text{cm})}{6(0.01\text{poise})} = 36.5\text{ml/min}$$

where τ – shear stress, H – spacer thickness, b – window length
μ – media viscosity

Microscopy

Following static and dynamic treatments, all PVA specimens are fixed with a 10% formalin solution for 24 hours and stained with hematotoxylin (primarily nuclear binding) using the drop method. A Retiga 1300 microscope system and Q Capture software application (provided by Q Imaging, Inc.) are used to estimate the confluence, morphology, and number of BAEC on the PVA specimens.

2.3 cHRSEM study of PVA hydrogels

Cryo-high resolution scanning electron microscopy (cHRSEM) is a powerful method for analyzing the physical properties of hydrogels. The use of this technique allows for observation of the polymeric network of the PVA hydrogel in the water-swollen state. Unlike traditional SEM, sample preparation conserves the natural state of the polymer through combined processes of water vitrification and sublimation, thus creating a faithful representation of material topology [43,44]. Controlled temperature fluctuations are used to sublime away loosely bound water from the sample surface in an etching process, while a subsequently applied vitrification process preserves the water that is intimately bound in the hydrogel. Magnification of up to 50,000X provides nanometer resolution and reveals the polymeric network of the hydrogel. A morphological characterization of the network in the natural, water-swollen state increases understanding of the molecular interactions that define the physical and mechanical properties of the PVA hydrogel.

Two PVA hydrogel samples (A, B) are prepared for observation with cHRSEM. The composition and processing parameters for each sample are described below.

Sample A:

Composition: 10% PVA (average M_w 124,000 – 186,000, provided by Aldrich Chemical Company, Inc), 90% DI, filtered H_2O.

Processing: Autoclave mixture on a liquid cycle with a chamber temperature of 121°C and a sterilization time of 25 minutes. Cast 1.5 ml of the resultant clear, homogeneous solution into each well of a 12-well polystyrene tray (well diameter of 2.54 cm). Expose the sample tray to a freeze/thaw (freeze at –20.0°C, thaw at

22°C) cycling scheme with the following time intervals: freeze for 8 hours, thaw for 4 hours, repeated 4 times consecutively. Remove samples from tray and store in DI, filtered H_2O at room temperature until cHRSEM study.

Sample B:

Composition: Similar to Sample A, with approximately a 20% PVA component.

Processing: Similar to Sample A, with a tubular mold configuration (mold configuration is irrelevant to this study). Also, the cycling scheme is slightly different for Sample B.

Note on Sample B: Sample B is provided by a biomaterials company, thus the particular compositional and processing parameters are kept confidential [42]. For the purposes of this study, the main difference between the two samples is taken to be PVA weight percentage.

Process used for cHRSEM study:

The following section is a summary of the process associated with hydrogel observation using cHRSEM [43].

1. Cut samples from solid-state, hydrated hydrogel source to fit in hemispherical gold planchet (3mm diameter).
2. Plunge freeze planchet in liquid ethane (-183ºC) for sample stabilization.
3. Transfer planchet with Teflon holders to a planchet holder that is stored in liquid nitrogen (-196ºC).
4. Evacuate cryopreparation stage (Gatan CT-3500) to 2 x 10^{-7} Torres.
5. Cool stage to -170ºC.
6. Load sample onto stage and fracture with prechilled blade.

7. Transfer to chromium coater (Denton DV-602) and raise temperature to -105ºC (sublimation and etching).

8. Chill down to -170ºC.

9. Coat with 2 nm film of chromium.

10. Transfer sample to microscope stage (-115ºC), allow 30 minutes for temperature stabilization.

11. Observe with in-lens field emission SEM (DS-130) with 25kV operating voltage.

CHAPTER 3

EXPERIMENTAL DESIGN

3.1 Mechanical characterization of PVA hydrogels

Uniaxial tensile testing of a strip

Uniaxial tensile tests are conducted on six formulations of PVA hydrogels. The purpose of these tests is to acquire the necessary stress-stretch data to propose a SEF for each of the PVA hydrogels.

'Dog bone' shaped samples of PVA hydrogels are used for uniaxial tensile testing with an EnduraTec ELF 3200 mechanical tester (Figure 1). This standard sample shape is used to minimize the effects of the stress concentrations in the grip-contacting region of the material. The middle segment of the sample has uniform cross-sectional area, and is assumed to undergo a uniform or very near to uniform reduction as the sample is subjected to tension.

The force-displacement data output for this uniaxial test is the instantaneous tensile force applied to the sample and the corresponding length of the uniform zone. This output, along with the initial geometrical measurements of the sample, is gathered for 6-8 samples of each material variation. This information is all that is required to propose a SEF for each of the six PVA hydrogel variations.

Uniaxial tensile testing of a ring

The combined purpose of this task and the next (tube inflation testing) is to provide the data for verification of a proposed SEF for a PVA hydrogel. The only material samples needed for these two tasks are uniform, thick-walled PVA hydrogel

tubes. The uniaxial tensile tests are conducted on ring samples formed from slices of the tubes, and provide the one-dimensional data required for a SEF analysis.

End pieces from three PVA hydrogel tubes are sliced to create six ring samples of similar dimension. A hook-like attachment is used correctly position the rings within the vice grips of the mechanical tester. The rings are exposed to uniaxial tension, with a recorded output of the instantaneous force and sample displacement. This output is then converted into the one-dimensional stress-stretch data needed to propose a SEF for this particular material formulation.

Tube inflation testing

Internal pressurization of a thick-walled tube represents a three-dimensional stress-strain state. The pressure-diameter data acquired from this experimental setup will be compared to the theoretical response based on the SEF developed from uniaxial tensile test of the same material. The effective use of one-dimensional data to predict a three-dimensional response will validate the SEF analysis of this PVA hydrogel.

A closed loop system is used to apply an internal pressure ranging from 0 – 600 mmHg to three PVA hydrogel tubes. The outer diameter of the tubes is measured at a pressure step of 50 mmHg. The collected experimental data are compared to the theoretical response of each tube, which are generated using the average one-dimensional stress-stretch response of the six ring samples and the undeformed tube geometry.

3.2 Feasibility study of cell adhesion to PVA hydrogels

The purpose of this study is to determine if a PVA hydrogel could support the adhesion of BAEC. Successful adhesion of BAEC would strengthen the feasibility of using PVA hydrogels as a cell seeding scaffold for tissue engineering applications, most notably the adhesion of human endothelium to promote blood compatibility in a vascular graft application. The effect of hydrogel surface roughness in the range of 0 – 250 microns is also analyzed. Samples are exposed to physiologic flow to determine if the cell adhesion strength is sufficient to withstand the stress environment of the native artery.

A 10 % PVA hydrogel is used to prepare various samples for cell seeding. The configuration of samples is shown in Figure 5. The white colored wells indicate the location of PVA samples that are to be coated with collagen and seeded with BAEC. The red colored wells indicate the location of BAEC seeded on collagen, which serve as a control to test the effect of the collagen. The yellow colored wells indicate the location of BAEC seeded directly onto the well surface, which serve as a control to test the health of the cells.

PVA hydrogel samples are prepared with the either smooth or rough surfaces as described in section 2.2. A 10% PVA solution is used to cast all samples, with the aforementioned temperature cycling scheme to facilitate physical crosslinking of the hydrogel. Following hydrogel formation, all samples are sterilized with a 24-hour exposure to UV light while immersed in H_2O (to prevent dehydration). A 1.0 ml collagen solution is applied to each sample and allowed to evaporate for 4 hours. Next, 1.0 ml of a

homogeneous BAEC suspension is applied to each well. The samples are then statically cultured for a 72-hour period in a standard incubation environment.

Cell confluence of the control wells is verified following the 72-hour incubation period. Each sample is then carefully bisected and labeled. One half of each sample is returned to the same static culturing environment for an additional 24-hours. The other half of each sample is used to generate 35 mm^2 rectangular specimens for dynamic treatment.

A physiologic flow loop is used to expose the 35mm^2 specimens to the shear stress arising in the native artery. The samples are subjected to a shear stress of 20 dyn/cm^2 for a 24-hour period. These samples, along with the other halves maintained in static incubation, are then simultaneously fixed with a 10% formalin solution for 24 hours. A nuclear staining procedure is performed to facilitate an adhesion rating of all samples with a Retiga 1300 stereomicroscope system. Cell count estimates and cell morphology ratings are then generated to evaluate the effect of surface roughness on BAEC adhesion to PVA hydrogels for both the static and dynamic treatments.

3.3 cHRSEM study of PVA hydrogels

cHRSEM is used to analyze two PVA hydrogel samples. Samples A and B have a 10% and 20% by weight PVA component, respectively. The distinguishing feature of this microscopic technique is the ability to capture the material in the hydrated, natural state. To accentuate this advantage, both samples were kept fully hydrated until the plunge freezing stage involving liquid ethane. The previously described methodology for using cHRSEM is applied to each of the samples. The resulting images are cataloged with reference to magnification, etching time and percent PVA composition.

CHAPTER 4

RESULTS AND ANALYSIS

4.1 Mechanical characterization of PVA hydrogels

Symbols

σ – Cauchy stress

F – force

A – deformed area

λ – stretch ratio

L – deformed length

L_0 – undeformed length

W – strain energy function (SEF)

I_1 – first Green strain invariant

I_2 – second Green strain invariant

ψ – response function of W

Φ – response function of W

P – applied internal pressure

A – linear regression coefficient

B – linear regression coefficient

a – dimensionless material parameter

c – stress-like material parameter

r – correlation coefficient

C – deformed ring circumference

C_0 – undeformed ring circumference

w_0 – undeformed ring width

t_0 – undeformed ring thickness

g – deformed grip separation distance

g_0 – undeformed grip separation distance

Uniaxial tensile testing of a strip

Uniaxial tensile tests are conducted on dog bone-shaped specimens with various processing and compositional parameters. The direct outputs of this experimental setup are force and displacement measurements, which are recorded by the mechanical tester. The first step in the analysis is to convert the force and displacement outputs into the stress and stretch ratio arising in the middle, uniform segment of the samples. Since PVA hydrogels undergo large deformations, the Cauchy stress is most appropriate for these calculations. The following equations are used to calculate Cauchy stress and stretch ratio.

$$\sigma = \frac{F}{A}$$

$$\lambda = \frac{L}{L_0}$$

For each given material variation, 6 – 8 PVA hydrogel samples are used to generate a plot of the stress versus stretch ratio for a stretch ratio range of approximately 1 - 2. The determined relationships are clearly nonlinear, and are pictured in Figures 6a - 6f. The error bars shown in these plots represent plus or minus 1 standard deviation from the average stress of like samples at each given stretch ratio. These plots provide descriptive data, but are not useful for predicting any other type of mechanical response involving these materials. To achieve mechanical characterization, subsequent analysis is focused on identifying the SEF of the materials.

Basic material assumptions about the mechanical response of PVA hydrogels include elasticity, homogenity, isotropy, and incompressibility. These assumptions are reasonable in light of the observed mechanical response in uniaxial tension, material processing methods, and material composition. The general case for such a material is that a SEF exists and is a function of the first two invariants of the strain tensor. The general form of the SEF is thus represented as $W = W(I_1,I_2)$.

The one-dimensional constitutive equation that follows from this general form is as follows:

$$\sigma = \left[\lambda^2 - \frac{1}{\lambda}\right]\left[\Phi(I_1, I_2) - \frac{1}{\lambda}\Psi(I_1, I_2)\right]$$

where $\Phi(I_1, I_2) = 2\frac{dW}{dI_1}, \quad \Psi(I_1, I_2) = -2\frac{dW}{dI_2}$ are the so called response functions

It is important to note that this equation contains two response functions, which are functions of the strain invariants. Evidently, the stress-stretch data from a uniaxial tensile test are insufficient to identify these two response functions.

However, if one of the two response functions is zero, the one-dimensional data are sufficient to quantify the SEF. Therefore, a further assumption about PVA hydrogel material class is required. Many synthetic materials, such as rubbers and silicon, which featuring long-range molecular order, belong to the material class with a SEF of the form $W = W(I_1)$. Also, biologic materials, such as elastin and the arterial wall, are considered to be in this material class. It is hypothesized in this study that the SEF of PVA hydrogels also depends on only the first invariant of the strain tensor, with the one-dimensional constitutive equation reducing to the following form.

$$\sigma = \left[\lambda^2 - \frac{1}{\lambda}\right]\left[\Phi(I_1, I_2)\right]$$

where $\Phi(I_1, I_2) = 2\dfrac{dW}{dI_1}$, $\quad \Psi(I_1, I_2) = -2\dfrac{dW}{dI_2} = 0$ are the response functions

This form of the one-dimensional constitutive equation and data from the uniaxial tensile tests are now used to solve for the only non-zero response function, as shown below.

$$\frac{dW}{dI_1} = \frac{\lambda\sigma}{2(\lambda^3 - 1)}$$

Notice that all the quantities on the right hand side of this equation can be calculated for at any state with data from the uniaxial test. The first invariant, I_1, is also obtainable from the one-dimensional data, as shown below.

$$I_1 = \lambda^2 + \frac{2}{\lambda}$$

A plot of dW/dI_1 versus I_1 could reveal information about the analytical form of SEF for PVA hydrogels. A linear form for the SEF is commonly used for materials of the class $W = W(I_1)$, which are termed neo-Hookean solids. The data obtained from the uniaxial tests on PVA hydrogels, however, do not suggest this functional form. Instead, exponential relationships between stresses on strains are manifest. With this in mind, a plot of $\ln(dW/dI_1)$ versus I_1 is generated for all material variations. A linear relationship between these two variables would indicate that an exponential form is appropriate for the SEF. As seen in Figures 7a - 7f, a linear relationship (average $R^2 > 0.95$) is indeed found for all tested PVA hydrogel variations. Linear regression of $\ln(dW/dI_1)$ versus I_1 yields:

$$\ln[\frac{dW}{dI_1}] = AI_1 + B$$

where A and B are the parameters of the linear regression.

Having in mind that for the initial undeformed state $\lambda = 1$ and $I_1=3$ and the corresponding value of W has to be equal to zero, it follows that the SEF has the form

$$W = \frac{c}{a}\left(\mathrm{e}^{a(I_1-3)} - 1\right)$$

where *c* and *a* are material constants related to the parameters of the linear regression as follows.

$$a = A$$
$$c = e^{(3A+B)}$$

Similar SEF form has previously been used to describe human carotid arteries, and is able to account for tissue stiffening effects observed in high stress regions [45].

Therefore, the form and material parameters for the proposed SEF are both extracted from the data plotted in Figures 7a - 7f. The same equation form is kept for the SEF of all material variations, with identification of the material parameters from the slope and intercept of the linear regression of $\ln(dW/dI_1)$ versus I_1. The material parameters of the six PVA hydrogel variations are shown in Table 2. No physical meaning is imbedded within the values of these parameters; they are only applicable to the form of the proposed SEF.

As a first pass verification of the proposed SEF, the one-dimensional constitutive equation and the material parameters are used to describe the response of the PVA hydrogels is uniaxial testing. A theoretical plot of stress versus stretch ratio of the materials in uniaxial tension is generated with the following expression of the one-dimensional constitutive equation.

$$\sigma_1 = 2c\left(\lambda_1{}^2 - \frac{1}{\lambda_1}\right)\exp\left[a\left(\lambda_1^2 + \frac{2}{\lambda_1} - 3\right)\right]$$

Figures 8a - 8f display comparative plots of the theoretical and experimental one-dimensional stress versus stretch ratio for the six material variations. The following equation is used to calculate the correlation coefficient between the theoretical and experimental curves.

$$r_{th-\exp} = \frac{\sum_{i=1}^{20}(\sigma_i^{th} - \sigma_{avg}^{th})(\sigma_i^{\exp} - \sigma_{avg}^{\exp})}{\sqrt{\sum_{i=1}^{20}(\sigma_i^{th} - \sigma_{avg}^{th})^2}\sqrt{\sum_{i=1}^{20}(\sigma_i^{\exp} - \sigma_{avg}^{\exp})^2}}$$

where the ‘th’ and ‘exp’ superscripts correspond to theoretical and experimental stress values, respectively, and the ‘i’ counter on the summations refers to the 20 incremented stretch ratios between 1 and 2 (step of 0.05).

An excellent correlation is observed for all material variations ($r_{th\text{-}exp} > 0.98$), indicating that the proposed SEF can effectively predict the one-dimensional response of the PVA hydrogels. However, this analysis is merely using one-dimensional data to predict a one-dimensional response. Further and more meaningful verification of the proposed SEF will involve the prediction of a more general mechanical response.

Uniaxial tensile testing of a ring

Ring samples sliced from PVA hydrogel tubes are subjected to uniaxial extension. A ring is positioned in the mechanical tester with hook fixtures at the top and bottom grips. The one-dimensional data gathered for the ring samples is processed as the previously described strip samples, with the following equations to calculate sample stress and stretch ratio.

$$\sigma = \frac{FC}{2w_0 t_0 C_0}, \qquad \lambda = \frac{C}{C_0} = \frac{2g + \pi a_0}{2g_0 + \pi a_0}$$

The Cauchy stress versus stretch ratio is shown in Figure 9, along with the error bars to denote plus or minus 1 standard deviation of the data gathered for the 6 ring samples. The one-dimensional response is similar in shape to that observed for the previous six material variations, but with indication of a somewhat stiffer material. A plot of $\ln(dW/dI_1)$ versus I_1 indicates that the same exponential form is appropriate to propose a SEF for this material, with a linear regression coefficient of 0.95. Figure 10 displays this plot along with the linear regression used to estimate the material parameters. Based

on the coefficient-parameter transform, the following material parameters are calculated for the ring samples.

$$a = 0.4473$$
$$c = 214.33\,kPa$$

These material parameters and the one-dimensional constitutive equation are used to generate a theoretical response of the ring samples. Figure 11 compares the theoretical and experimental one-dimensional response of the ring samples. Once again, excellent correlation ($r_{th\text{-}exp} > 0.99$) is found with this type of evaluation. The next step is to use the SEF already determined to solve a boundary value problem for a thick-walled tube subjected to internal pressure and held at constant axial length.

Tube inflation testing

Internal inflation of a thick-walled tube is used to determine the three-dimensional response of a PVA hydrogel. The external diameter at stepped increases of internal pressure is measured using a closed loop system. The internal pressure versus external diameter is plotted for three tubes, as shown in Figures 12a - 12c. The error bars in these plots denote plus or minus 1 standard deviation of 6 measurements taken at each incremental pressure on a given tube. The tubes are composed of the same material as the ring samples used in previous experimentation, and should be characterized by the proposed SEF and material constants. To validate the proposed SEF, a theoretical internal pressure versus external diameter curve is generated and compared to the experimental results.

When considering the three-dimensional model of an inflated tube in this test setup, the conditions of axisymmetric deformation and plane strain are assumed. The plane strain assumption means that all the deformation occurs in a single plane, namely

the plane composed of the radial and circumferential directions. There is no deformation imposed in the axial direction. The equation presented below follows from the integration of the equilibrium equation of a thick-walled tube in the radial direction after imposing the boundary conditions that the tube is inflated by an internal pressure P and no load is applied on the outer surface.

$$P = 2\int_{r_i}^{r_e} \frac{dW}{dI_1}\left(\lambda_\theta^{\,2} - \lambda_r^{\,2}\right)\frac{dr}{r}$$

where the 'i' and 'e' subscripts refer to the internal and external deformed tube radii, respectively, and the 'θ' and 'r' subscripts refer to the circumferential and radial stretch ratios, respectively [46].

Although this integral equation is complicated, it can be solved numerically because all of the integrated variables are completely described by a single ratio of deformed to undeformed tube radii [46]. A Pascal IV computer program offered by Dr. Rachev is used to predict the inflation of a thick-walled tube based on the three-dimensional constitutive and equilibrium equations and the proposed SEF. The program inputs include the material parameters, the tube dimensions, the axial stretch of the tubes (no stretch applied), and the internal pressure. The program output of interest is the external radius of the tube, which is easily converted into external diameter. Figures 13a - 13c show comparative plots of the theoretical and experimental inflation of the three PVA hydrogel tubes.

High correlation ($r_{th\text{-}exp} > 0.99$) is noted between the theoretical and experimental curves for all three tubes, indicating the precision of the proposed SEF. However,

differences between the theoretical and experimental curves are evident, especially at higher internal pressures. A comparison of linearizations of the curves reveals somewhat different slopes between the graphs. On average, there is about a 5% difference in the linearized slopes of the experimental and theoretical curves for the three tubes. This lack of accuracy is attributed to both one- and three-dimensional experimental limitations and is addressed in subsequent sections.

Considering the results of this verification procedure, the proposed SEF classification of $W = W(I_1)$ is accepted for PVA hydrogels. The actual material parameter values determined predict deformation curves that correlate well with experimental values, although some lack of accuracy must be accounted for through experimental limitations. Overall, the constitutive approach is an appropriate and convenient method to mechanically characterize PVA hydrogels.

4.2 Feasibility study of cell adhesion to PVA hydrogels

The findings of this study demonstrate that BAEC can adhere to the surface of a PVA hydrogel and suggest that this material can potentially provide a support scaffold for an endothelial cell monolayer in a load-bearing, tissue-engineering application. Furthermore, the presence of hydrogel surface roughness in the range of 27- 250 μm is shown to enhance the mean BAEC adhesion strength.

Various PVA specimens are seeded with a homogeneous cell suspension and identical technique at the onset of a static 72-hour culture period. Six samples of each surface roughness are then labeled and cut in half for two differential culturing treatments. The first treatment is a continuation of static culturing for a 24-hour period. The second treatment is a 24-hour exposure to arterial-like shear stress in the previously described physiologic flow loop (dynamic treatment). A BAEC count over an area of 25,400 μm^2 is taken for all samples and is summarized in Figure 14.

Each dynamic specimen is then compared to its static counterpart to generate an estimate of the percentage of BAEC that are able to remain adherent following the dynamic treatment. This analysis assumes that an approximately homogeneous cell seeding density is present on the PVA specimens prior to the differential culturing treatments. Figures 15 and 16 display samples and averages of this comparison for the 5 different surfaces, respectively. The error bars in Figure 16 denote the standard deviation of this data.

Figure 16 suggests that the presence of surface roughness on the hydrogel surfaces led to an enhancement of BAEC adherence following the dynamic treatment. Although the differences did not reach statistical significance between the smooth surface and three of the micro-topographies (27μm, 85μm, and 250μm), a notable improvement is seen in the 149 μm roughness samples (Figure 17).

A morphological assessment of the BAEC adherence is made for all specimens. Specimens are rated on a scale of 1 – 3, with 1 corresponding to the flatten morphology (indicating global cellular adherence), 2 corresponding to an intermediate level of adherence, and 3 corresponding to a spherical morphology (indicating adherence through an isolated focal adhesion site). Examples and results of this assessment are displayed in Figures 18a - 18c and Table 3, respectively.

Figure 18a displays BAEC with a flattened morphology, indicating the presence of extensive cell/surface interaction through a protein intermediate. Such morphology is standard in the intimal layer of the arterial wall. Figure 18c depicts rounded cells that are indicative of incomplete and fleeting adherence. This level of adherence is not sufficient for a tissue engineering application that is dependent on EC functionality. In general, the PVA hydrogel samples featuring surface roughness improved the average cellular morphology over the smooth samples (Table 3). The 149μm samples displayed the healthiest average morphology for both static and dynamic treatments.

Overall, the results of this study suggest that the 149μm square grid surface roughness pattern provided a preferential topography for BAEC adhesion to PVA hydrogels in the roughness range tested. This information can motivate and guide future research focused on the clinically relevant adhesion of human endothelium to PVA

hydrogels. BAEC adhesion provides a convenient animal model to project the possibility of seeding a monolayer of human EC to a given surface. The optimal surface conditions may differ for bovine and human endothelium, and that a more favorable PVA hydrogel surface roughness could be identified for HEC adhesion.

4.3 cHRSEM study of PVA hydrogels

A cHRSEM study of two PVA hydrogels provides three-dimensional, high magnification images of the material surfaces. Figures 19a and 19b displays these images, which have been organized based on the PVA hydrogel sample (A or B), the magnification, and the etch time.

The only parameter of the cHRSEM process that is varied in obtaining these images is the etching time. The etching away of loosely-bound bulk water from the material surface is accomplished using a ramped temperature elevation from -170 ºC to -105 ºC in an evacuated environment (2×10^{-7} Torres). The effect this process has on the material surface is the sublimation of a supposed hydration shell, which then exposes the uniform matrix of the polymer network for vitrification [43].

This study explores three different etching times to treat the PVA hydrogels. A 5-minute and 3-minute etch time, along with a no etch run, are all attempted. The 5-minute etch run yields useless images, as seen in Figure 19a. This elongated etching period is hypothesized to have completely sublimed away any existing material hydration shell and also distorted the water that is tightly bound to the PVA molecules. These distorted images picture a glassy or smooth surface for the hydrogels even at high magnification, which suggests the occurrence of polymer network degradation followed by a disorganized material reconstitution.

The 3-minute etch time yields slightly better images, indicating that reducing the etch time further would improve the network resolution. As seen in Figure 19a, the 3-minute etch begins to reveal the polymeric components of the PVA hydrogel. A

honeycomb-like pattern is visible in different regions of the sample surface, indicating that this is an actual portrayal of the polymer network.

The final run on the PVA hydrogels bypasses the etching period and views the material with any existing hydration shell left undisturbed. As seen in Figure 19b, this procedure modification produces excellent high magnification images of the material surface. This result suggests the amount of free water that remains as bulk is minimal; most or perhaps all of the water incorporated into PVA hydrogels bonds intimately with the polymer network. This conclusion is consistent with the mechanical properties observed for PVA hydrogels, which include high strength and low compressibility.

CHAPTER 5

DISCUSSION

5.1 Implications of results for synthetic vascular grafts

The described experimentation is motivated by the current deficiencies in synthetic vascular graft technology. Thrombogenisis and intimal hyperplasia are the two main responsive phenomena that limit the size and efficacy of synthetic vascular grafts. Numerous possible strategies are being explored to mitigate these problems, leading to the emergence of new candidate biomaterials and methodologies.

PVA hydrogels are very promising materials for almost any load-bearing biomaterial application, including vascular grafts. Mechanical characterization, cell adhesion feasibility, and cHRSEM imaging are useful studies to further the appropriation of PVA hydrogels for graft development. The particular implications of each area of research are described below.

Mechanical characterization

The main benefit of a mechanical characterization to graft development is facilitation of structure design and analysis. Knowledge of the SEF and constitutive equations for PVA hydrogel allows for accurate calculation of the stress-strain state of a graft placed under physiologic loads, as needed to rate performance. Furthermore, the stress-strain state of a graft is relevant to adherent cells, with cell types such as SMC displaying mechanosensitivty. The occurrence of intimal hyperplasia is correlated to both compliance mismatching between the graft and the native artery and to the recurring stretching of a graft during the cardiac cycle. An understanding of the stress-strain

response of a PVA hydrogel will be useful in the design of vascular grafts to control intimal hyperplasia and improve graft efficacy.

A comparison of the tested PVA hydrogel tubes to arterial compliance data collected from humans ranging from 40 – 59 years old is shown in Table 4 [47]. The following equation is used to calculate the compliance of a PVA hydrogel tube and the various vessels.

$$C = \frac{(D_s - D_d)}{(P_s - P_d)D_d} \times 10^{-2} \quad [\frac{\%}{mmHg}]$$

where C is compliance, D_s and D_d are the external diameters at systole and diastole, respectively, and P_s and P_d are the internal pressures at systole and diastole, respectively.

Although the hydrogel tube tested in this experiment is approximately one order of magnitude less compliant than the comparative vessels, adjustment of the compositional and processing parameters could likely lead to a compliance-matched graft. In fact, using the SEF and material parameters identified for the 10%, 6 cycle PVA hydrogel, a compliance of 0.27 %/mmHg is calculated for tubes with an undeformed external diameter of 8 mm and wall thickness of 1 mm for pressures of 80 and 120 mmHg. The compliance of this PVA hydrogel is bracketed by the presented clinical data, which further validates these materials as promising graft candidates.

Cell adhesion feasibility study

Platelet activation is one of the first known events that leads to thrombus formation. With the potential for graft occlusion, the importance of negating or minimizing this activation is clear. To date, a synthetic surface with this ability is not known. A leading strategy to minimize platelet activation is the use of an EC monolayer

on the inner surface of a graft. This mimicry of the native arterial tissue could be accomplished through *in vitro* endothelialization prior to implantation or *in vivo* recruitment and formation of an EC monolayer following implantation.

The cell adhesion feasibility study of PVA hydrogels demonstrates that these materials are likely to support the adhesion of HEC. Since BAEC adhere to the material surface *in vitro* with an adhesion strength to withstand physiologic flow, it is logical to conclude that a HEC monolayer could also form on this surface. The results of this study challenge previous conclusions that deem hydrophilic surfaces as poor substrates for cell and protein adhesion [48,49]. Futhermore, this study suggests that surface roughness is promising technique to promote this material-cell adhesion.

An indirect implication of this study is the proven ability of PVA hydrogels to absorb surface proteins. Each hydrogel surface is coated with a layer of Type 1 purified collagen prior to cell seeding. Without this protein incorporation into the material surface, subsequent cell adhesion is not possible. Experimentation not presented demonstrates that no BAEC adhesion occurs on PVA hydrogel surfaces without collagen treatment. Protein and peptide addition to a material surface is the main technique to promote cell recruitment following implantation. Due to the difficult issue of cell sourcing facing *in vitro* EC formation, this is an especially crucial point for vascular graft development.

cHRSEM imaging

High magnification imaging of a material surface enhances the understanding of why and how material-tissue interactions occur. The use of cHRSEM in this study demonstrates that it is an effective technique to analyze the surface of PVA hydrogels, especially when the bulk water etching procedure is omitted. Material characteristics

relevant to vascular graft design are dependent on the composition and processing of PVA hydrogels. Parameters such as porosity, network density, and fiber thickness can be compared for various PVA hydrogels using cHRSEM.

5.2 Experimental limitations

Research endeavors often require simplifying assumptions to generate results and the discretionary use of those results to avoid misconceptions. A description of the experimental limitations for each research area will facilitate the appropriate use of the obtained results.

Mechanical characterization

To completely describe the mechanical properties of PVA hydrogels, simplifying assumptions about the general material properties are made. In particular, PVA hydrogels are treated as elastic materials under rapidly changing loads, although they are probably viscoelastic. The homogeneity of the materials is taken for granted despite some visible regions of variable composition. The hydrogels are also considered incompressible materials based on their high water content.

In addition to assumptions about the material properties, other limitations are evident in experimental setup. During uniaxial strip testing, elongation of the material sample is indirectly measured based on the grip separation of the mechanical tester (displacement-controlled testing). If the tapered regions of the dog bone samples with variable thickness undergo deformation, then the force measured at any given stretch ratio is an inflated value. The extended length of the testing region of the dog bone shape is designed to minimize this effect. A 10:1 sample length to width ratio is standard for this test, but is not attainable with the available equipment. Due to the geometrical constraints of the testing load cell and grip apparatus and the intent to realize a stretch ratio of up to two for all samples, only a 5:1 ratio is possible. Although care is taken to

exclude or minimize the thicker regions from the test segment, this force overestimate likely persists to some degree.

The tube inflation testing presents some difficulties in sample placement. For accurate deformation measurements, the tube must be kept at constant length with zero axial strain. Furthermore, no twisting can be induced in the tube. In practice, it is almost impossible to attach the tube into the loop while strictly abiding by these guidelines. Although extreme care is taken for tube placement, incidental tube deformations probably occurred.

Despite some statistically significant discrepancies between theoretical and experimental data, the proposed SEF is accepted for PVA hydrogels. The high level of correlation between theoretical and experimental curves for both one- and three-dimensional testing indicates that the material classification is correct, although the evident lack of accuracy suggests experimental errors, which are attributed to the aforementioned limitations.

The resulting SEF and material parameters for each hydrogel variation also require careful interpretation. These mechanical characterizations are specific only to the tested material processing and compositional parameters. The actual values of the determined coefficients have no physical meaning or relation to the PVA hydrogels outside the scope of this analysis. Interpolation of material coefficients to characterize any untested PVA hydrogel is errant. The true value of this work is the SEF classification of PVA hydrogels ($W=W(I_1)$) and the demonstrated method of coefficient determination.

Cell adhesion feasibility study

The nature of *in vitro* cell adhesion studies limits their results to the chosen culture system and cell type. The conducted experiment is no exception, as the results are only descriptive of BAEC in a standard culture environment. The dynamically treated samples showing successful BAEC adhesion do not prove that an endothelium could form on PVA hydrogels *in vivo*. However, the results do show that this is feasible, and suggest surface roughness as a possible method for enhancing HEC adhesion.

In addition to the general limitations of *in vitro* studies, sources of error are found in the experimental methodologies. Although 7^{th} passage cells from the same line are the common source for all BAEC tested in the study, a difference in cell population health may have existed between the various culture flasks. Previous experimentation has shown visible variance between flask populations of the same passage with no evident explanation. Although the flask populations used in the study all appeared in equally good health prior to cell seeding, the possible existence of an undetectable differences between flasks is recognized.

Specimen preparation and analysis represent major sources of error in this study. Dynamically treated specimens are formed from 35 mm^2 slices from a larger area. These specimens are difficult to produce and handle, and any adherent BAEC are likely subjected to some incidental stress. BAEC counting and morphology estimates on the hydrogel surfaces are often highly speculative, and would differ based on the observer. Although unbiased methods are used for analysis, this necessary speculation is an inherent limitation of the study.

cHRSEM imaging

The cHRSEM images of PVA hydrogels are excellent for studying the surface of these materials. This study is mainly limited in scope, as the resulting images only depict 2 particular material variations. Due to the small number of facilities that have cHRSEM, it would be expensive to obtain similar images for any other material or conduct a comparative study.

5.3 Conclusions and recommendations

The conducted research is focused on the potential use of PVA hydrogels for vascular graft development. The results of the three separate studies all indicate that continuing research on this topic is valid and promising. Complete mechanical characterization of PVA hydrogels is attainable with data from a basic one-dimensional extension test, and provides future researchers with a powerful tool to design compliance matched grafts. The formation of an EC monolayer on the inner surface of a PVA hydrogel graft is shown to be feasible, and represents a possible strategy to diminish the thrombogenic response. cHRSEM depictions of PVA hydrogels in the natural, water-swollen state reveal great detail about the composition and topography of the material surface, and can help explain material-tissue interactions.

In the ongoing effort to develop suitable small diameter vascular grafts and improve the patency of existing grafts, PVA hydrogels demand thorough consideration. This work and others confirm that these materials are mechanically similar to native soft tissue and are biocompatible. The flexibility of PVA hydrogel preparation yields materials with a wide range of properties, making them applicable to various biomaterial and tissue engineering devices.

TABLES

Table 1: Sample number of PVA variations for uniaxial testing

	Percentage PVA	
Cycle Number	10	15
2	8	6
4	7	7
6	7	7

Table 2: Material parameters for proposed SEF

Coefficients of Linear Regression [ln(dW/dl) = A(l) + B]

A			B		
	Percentage PVA			Percentage PVA	
Cycle Number	10	15	Cycle Number	10	15
2	0.5471	0.4112	2	-0.1530	0.8154
4	0.6931	0.5112	4	0.4770	1.7374
6	0.6502	0.4204	6	0.887	2.2112

Coefficients of SEF [a=A, c=exp(3A+B) kPa]

a			c		
	Percentage PVA			Percentage PVA	
Cycle Number	10	15	Cycle Number	10	15
2	0.5471	0.4112	2	4.429	7.7597
4	0.6931	0.5112	4	12.888	26.338
6	0.6502	0.4204	6	17.087	32.214

Table 3: Summary of average morphological assessment with scale ranging from 1.00 (highest adhesion rating) to 3.00 (lowest adhesion rating)

Surface Roughness (microns)	Statically Treated	Dynamically Treated
0	2.50	2.33
27	1.17	2.67
85	1.16	1.33
149	1.00	1.17
250	1.17	2.17

Table 4: Compliance comparison of human arteries to PVA tube

Human (40-59 yrs)	Abdominal Aorta	Common Carotid Artery	Brachial Artery	Femoral Artery	PVA Hydrogel Tube 1
P_s (mmHg)	117	119	120	118	100
P_d (mmHg)	72	72	75	70	50
D_d (mm)	15.30	7.30	4.10	8.80	7.31
D_s-D_d (mm)	0.930	0.490	0.160	0.390	0.060
$(D_s-D_d)/D_d$	0.070	0.070	0.040	0.050	0.008
P_s-P_d (mmHg)	45	47	45	48	50
Compliance (%/mmHg)	0.15556	0.14894	0.08889	0.10417	0.01641

FIGURES

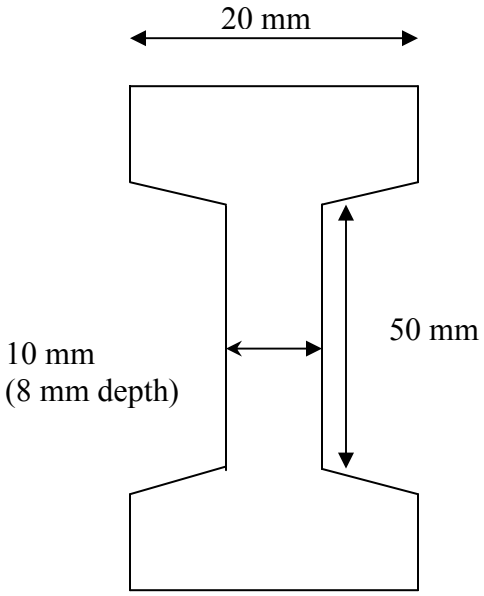

Figure 1: Schematic of dog bone-shaped samples for uniaxial tensile test

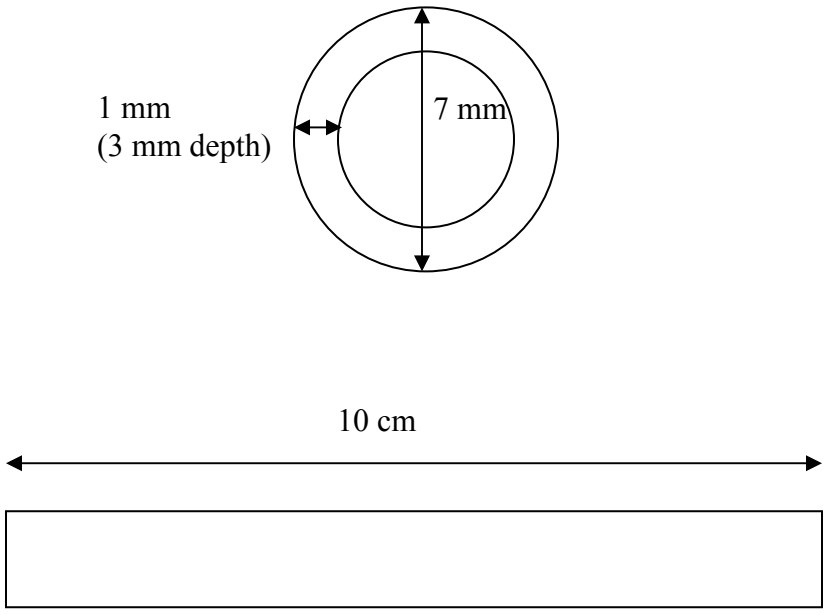

Figure 2: Schematic of samples for uniaxial tensile test of a ring and tube inflation test

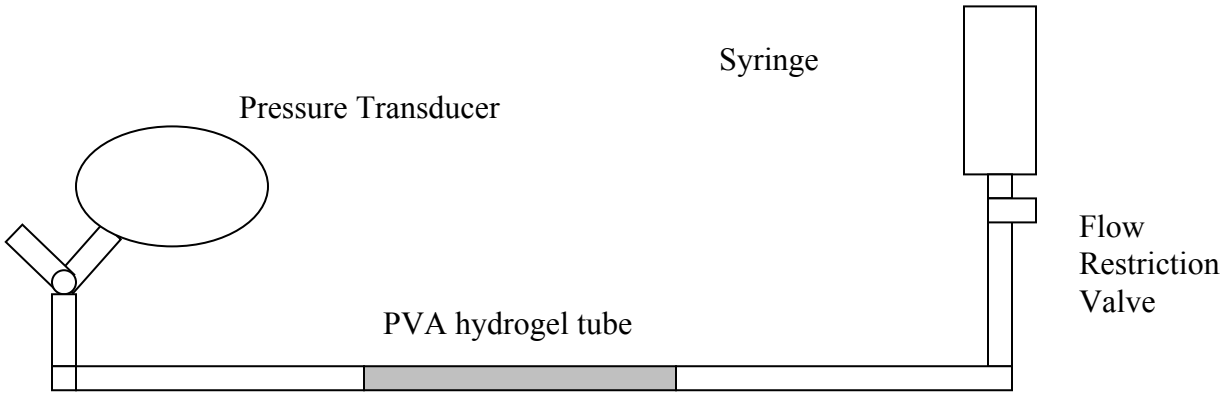

Figure 3: Schematic of closed loop for tube inflation testing

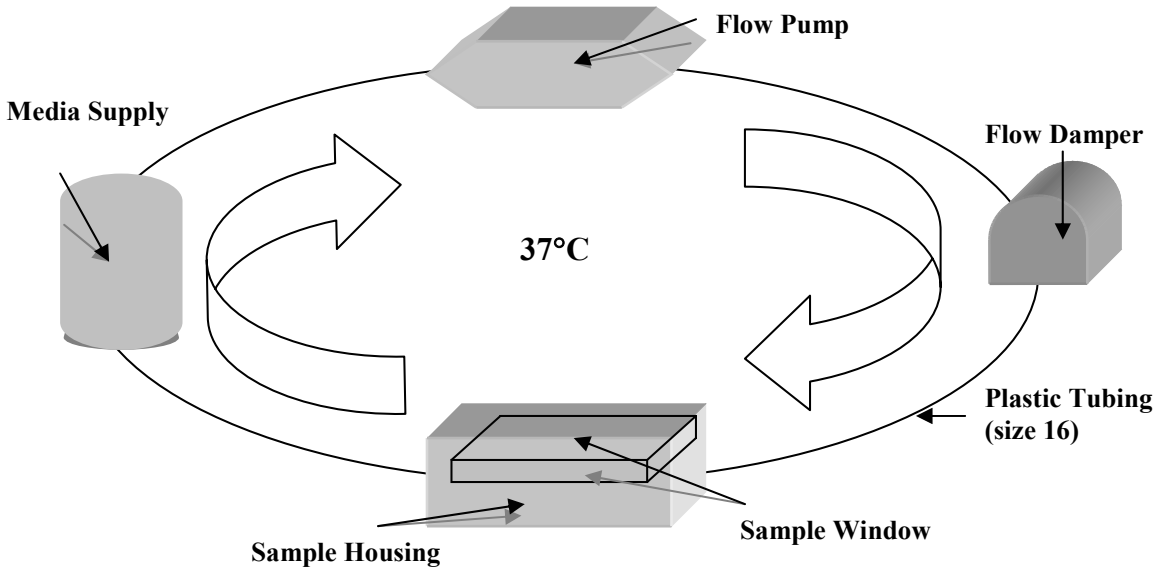

Figure 4: Schematic of physiologic flow loop

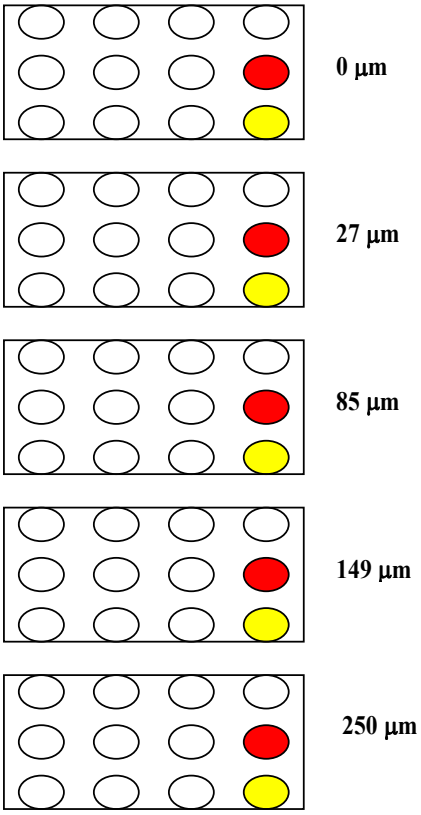

Figure 5: Configuration of wells for PVA hydrogel sample preparation

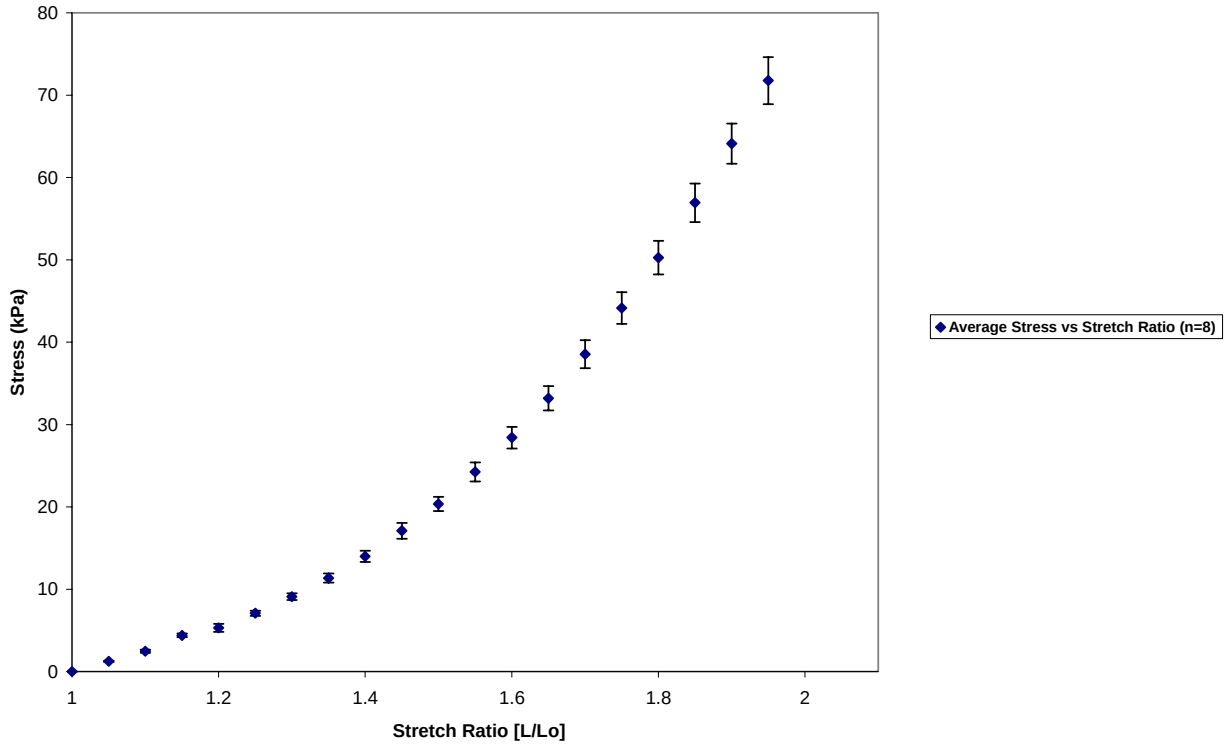

Figure 6a: Average experimental stress versus stretch ratio of a strip (10%, 2 cycle PVA hydrogel)

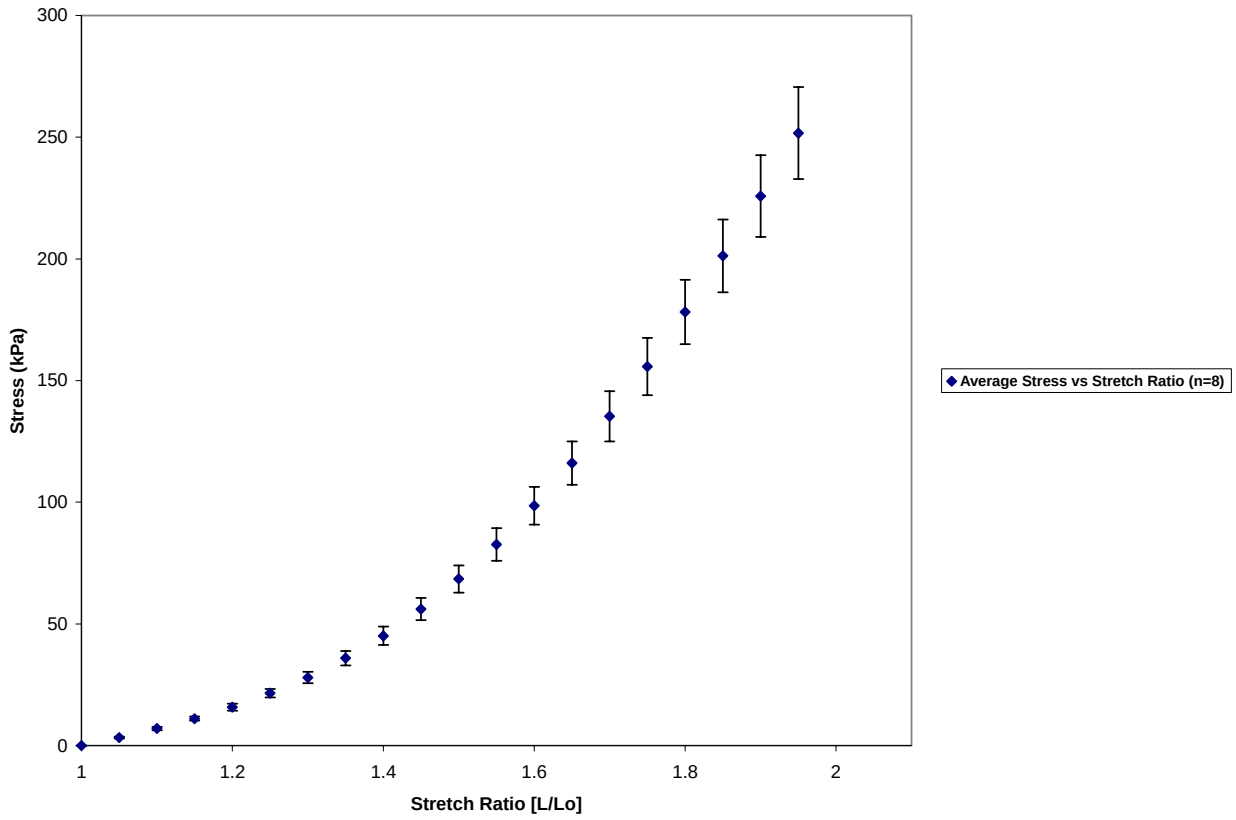

Figure 6b: Average experimental stress versus stretch ratio of a strip (10%, 4 cycle PVA hydrogel)

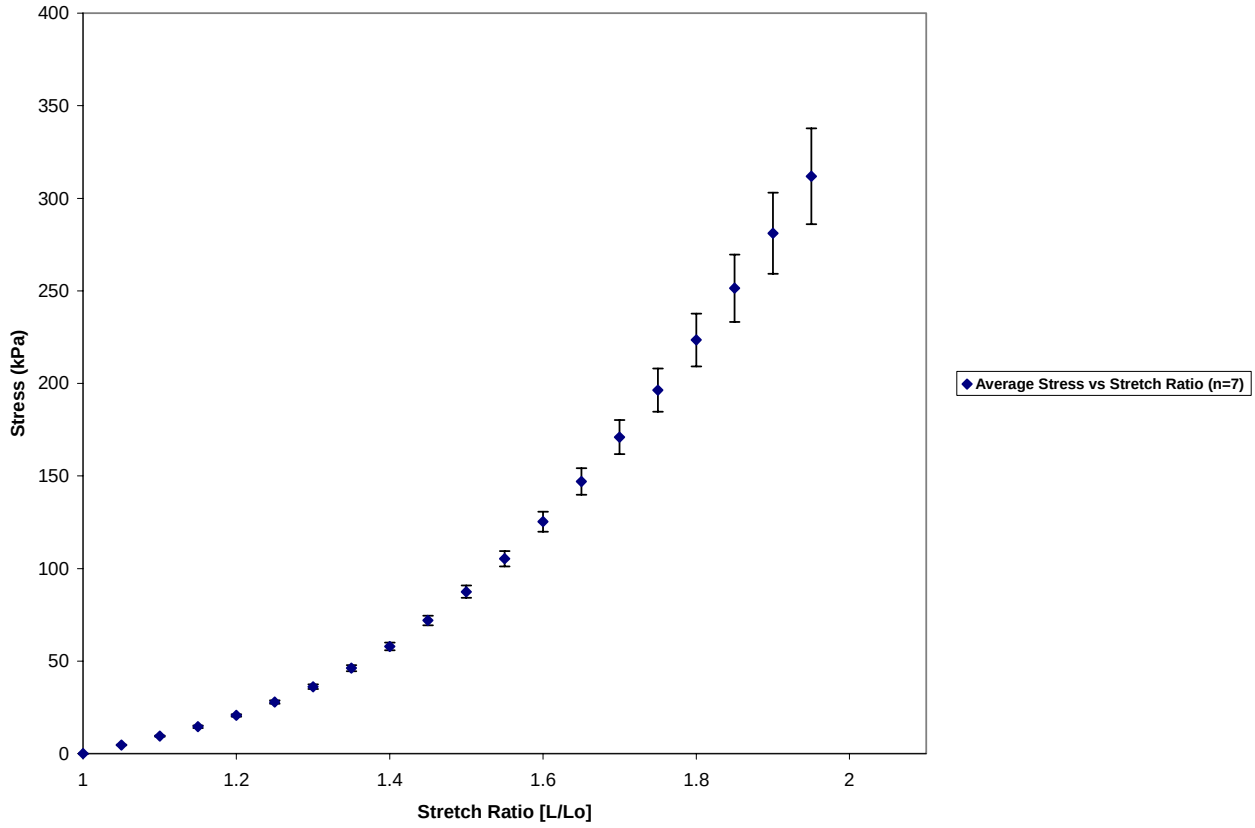

Figure 6c: Average experimental stress versus stretch ratio of a strip (10%, 6 cycle PVA hydrogel)

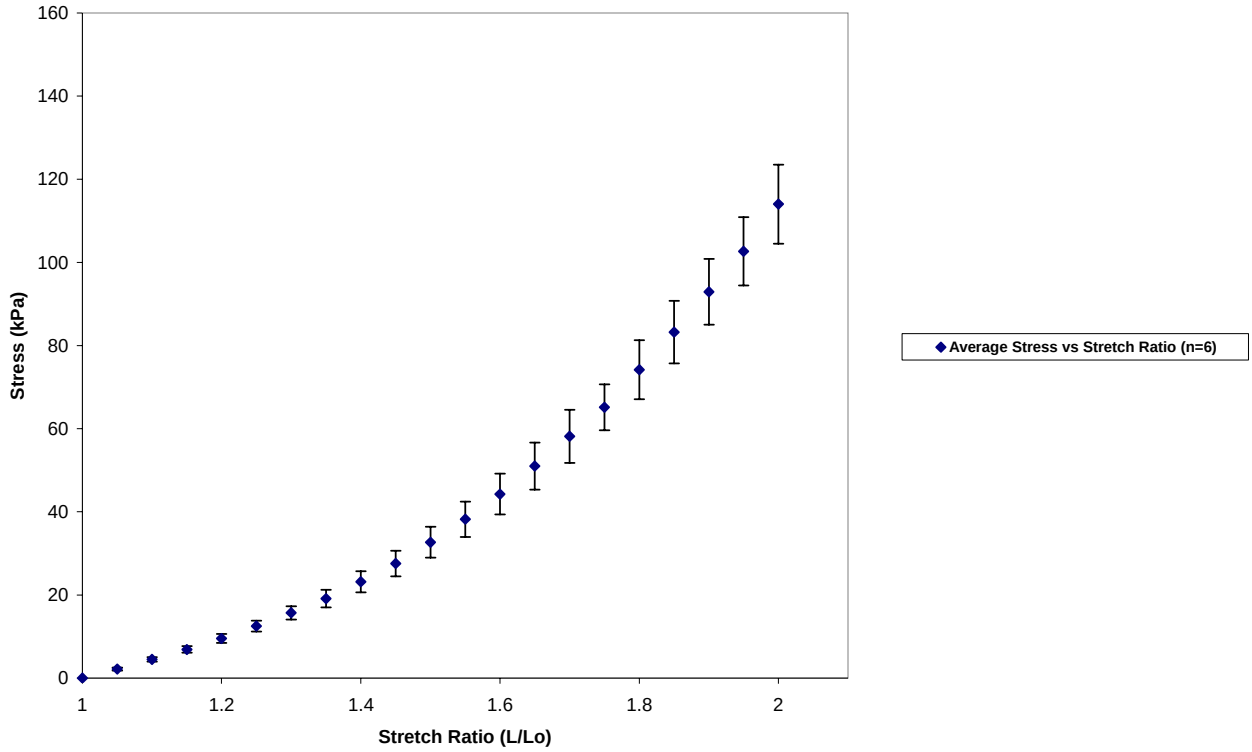

Figure 6d: Average experimental stress versus stretch ratio of a strip (15%, 2 cycle PVA hydrogel)

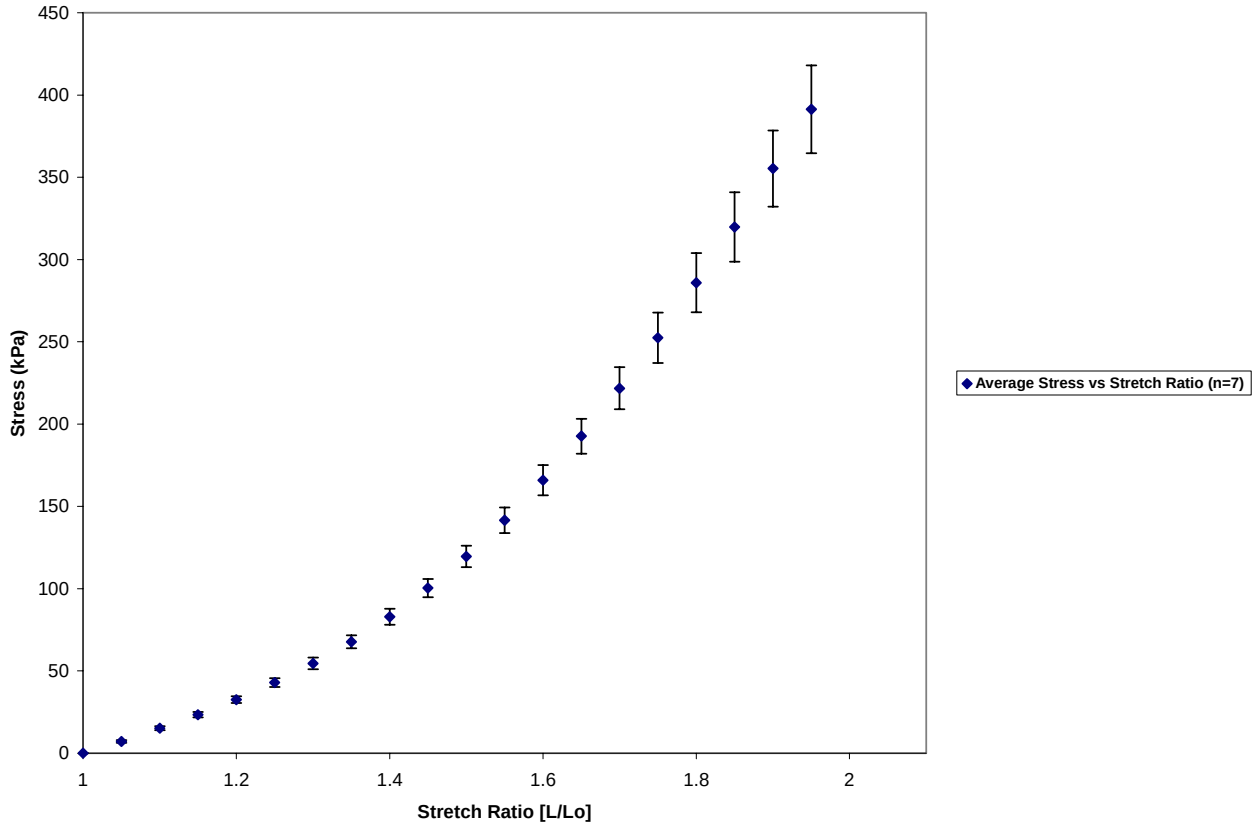

Figure 6e: Average experimental stress versus stretch ratio of a strip (15%, 4 cycle PVA hydrogel)

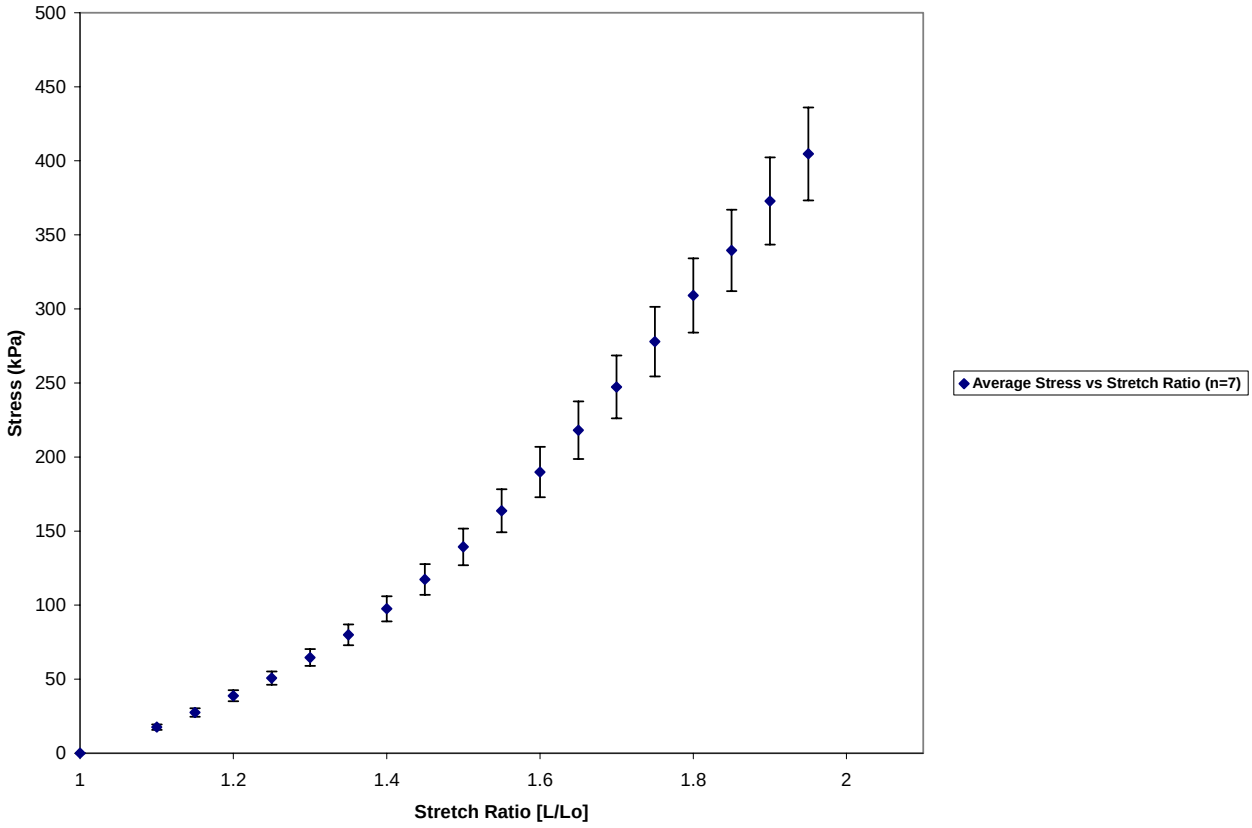

Figure 6f: Average experimental stress versus stretch ratio of a strip (15%, 6 cycle PVA hydrogel)

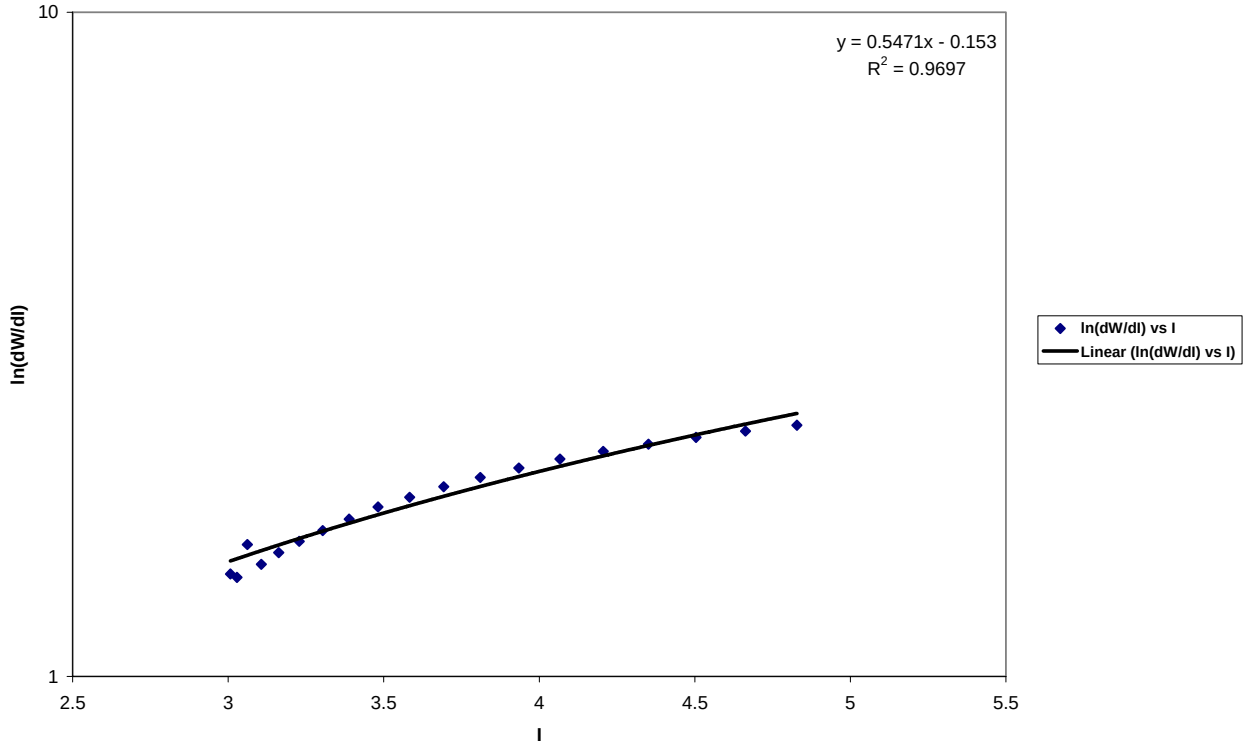

Figure 7a: Average experimental ln(dW/dI) versus I of a strip (10%, 2 cycle PVA hydrogel)

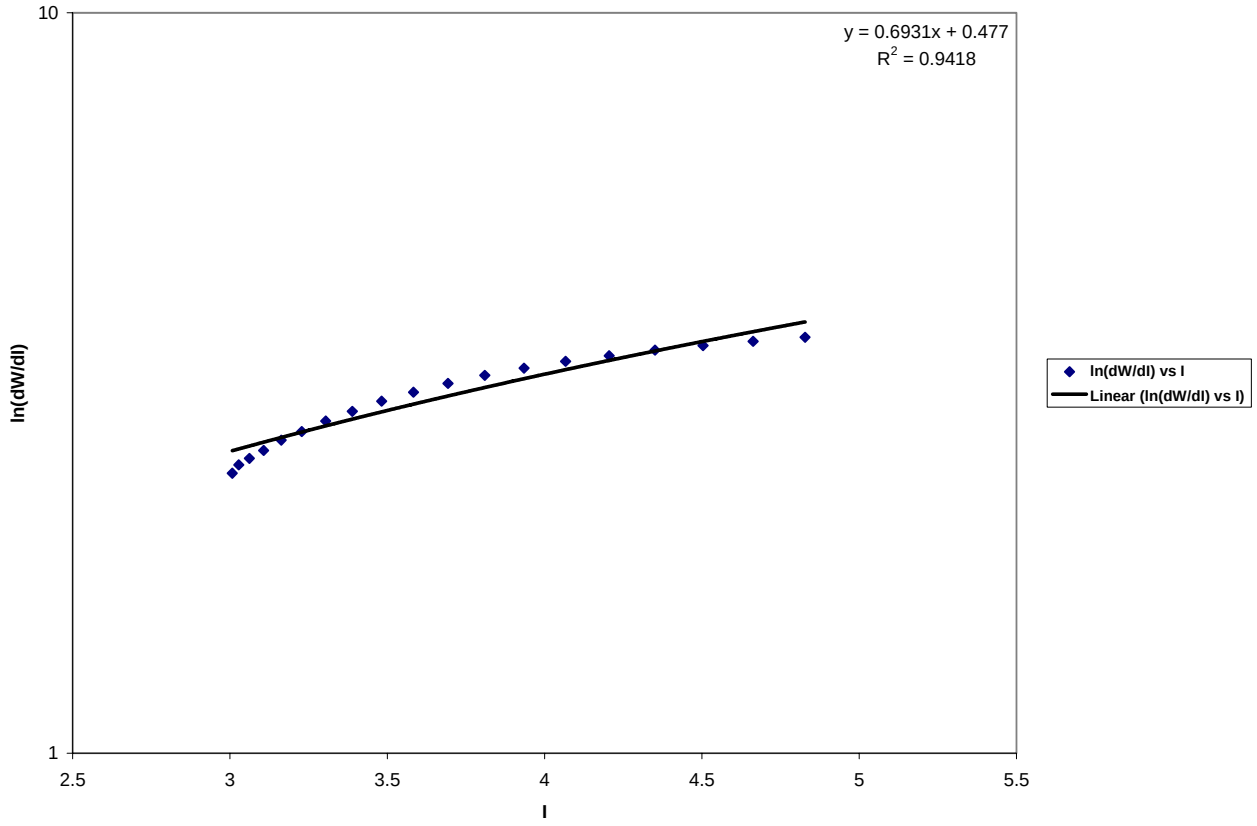

Figure 7b: Average experimental ln(dW/dI) versus I of a strip (10%, 4 cycle PVA hydrogel)

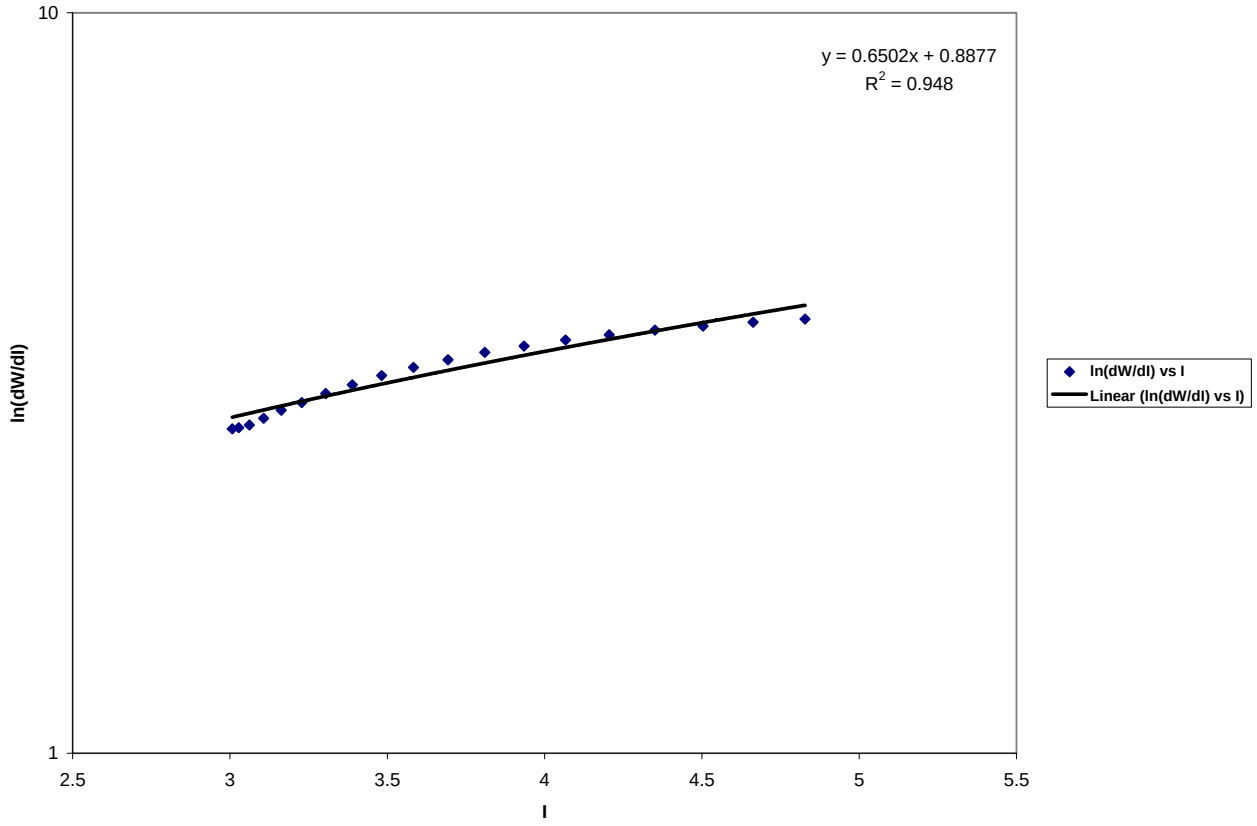

Figure 7c: Average experimental ln(dW/dI) versus I of a strip (10%, 6 cycle PVA hydrogel)

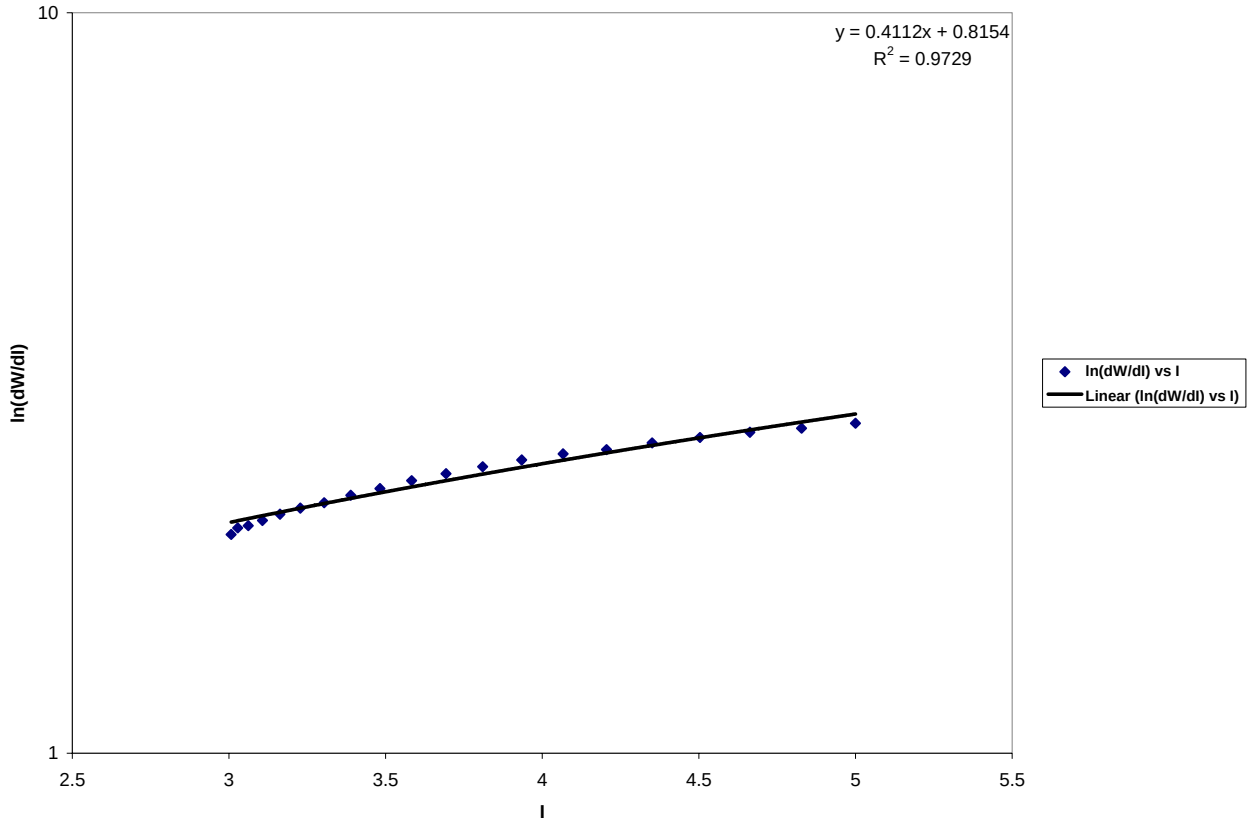

Figure 7d: Average experimental ln(dW/dI) versus I of a strip (15%, 2 cycle PVA hydrogel)

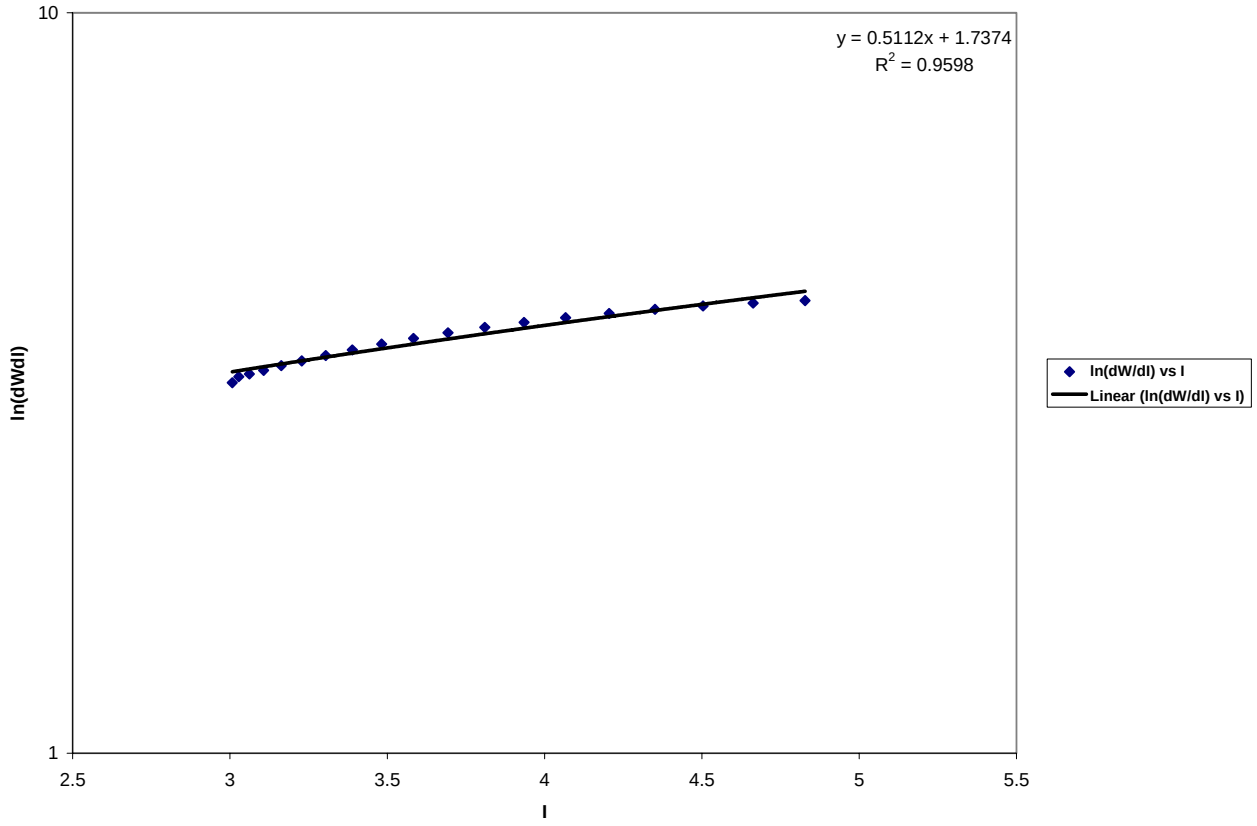

Figure 7e: Average experimental ln(dW/dI) versus I of a strip (15%, 4 cycle PVA hydrogel)

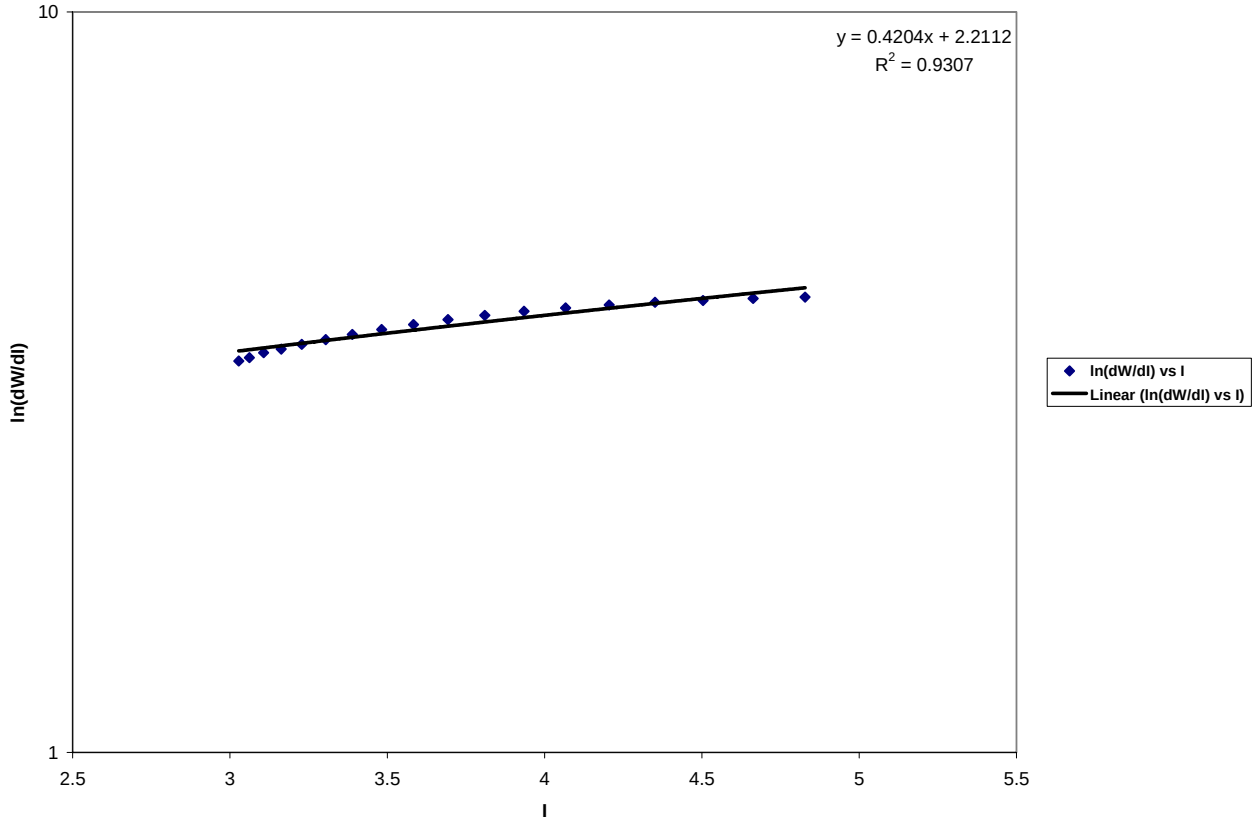

Figure 7f: Average experimental ln(dW/dI) versus I of a strip (15%, 6 cycle PVA hydrogel)

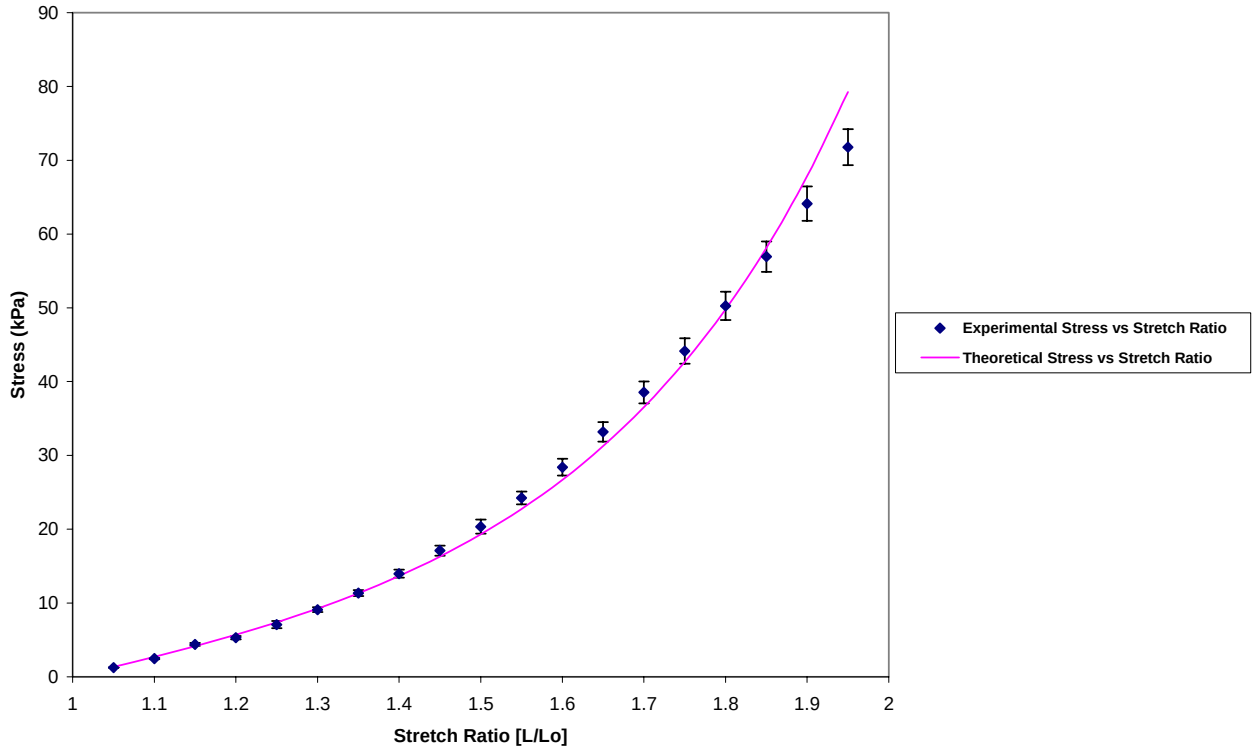

Figure 8a: Theoretical and experimental 1D response of a strip (10%, 2 cycle PVA hydrogel)

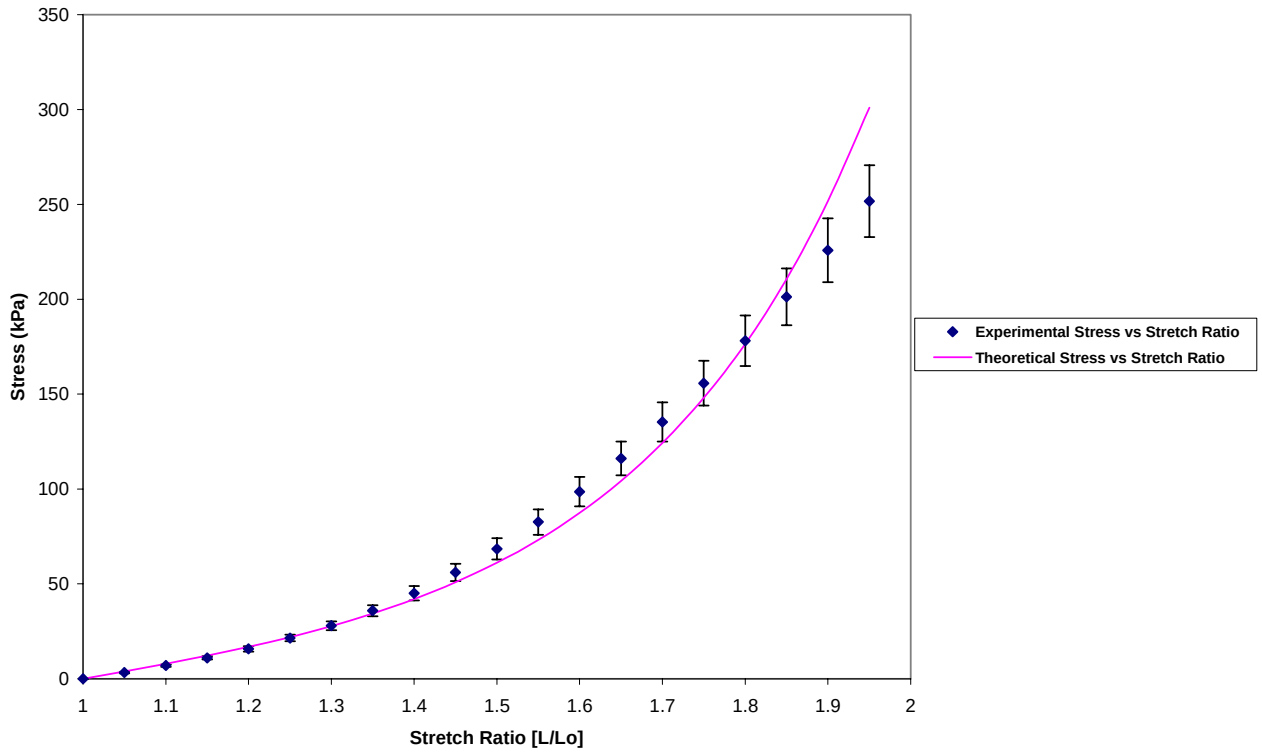

Figure 8b: Theoretical and experimental 1D response of a strip (10%, 4 cycle PVA hydrogel)

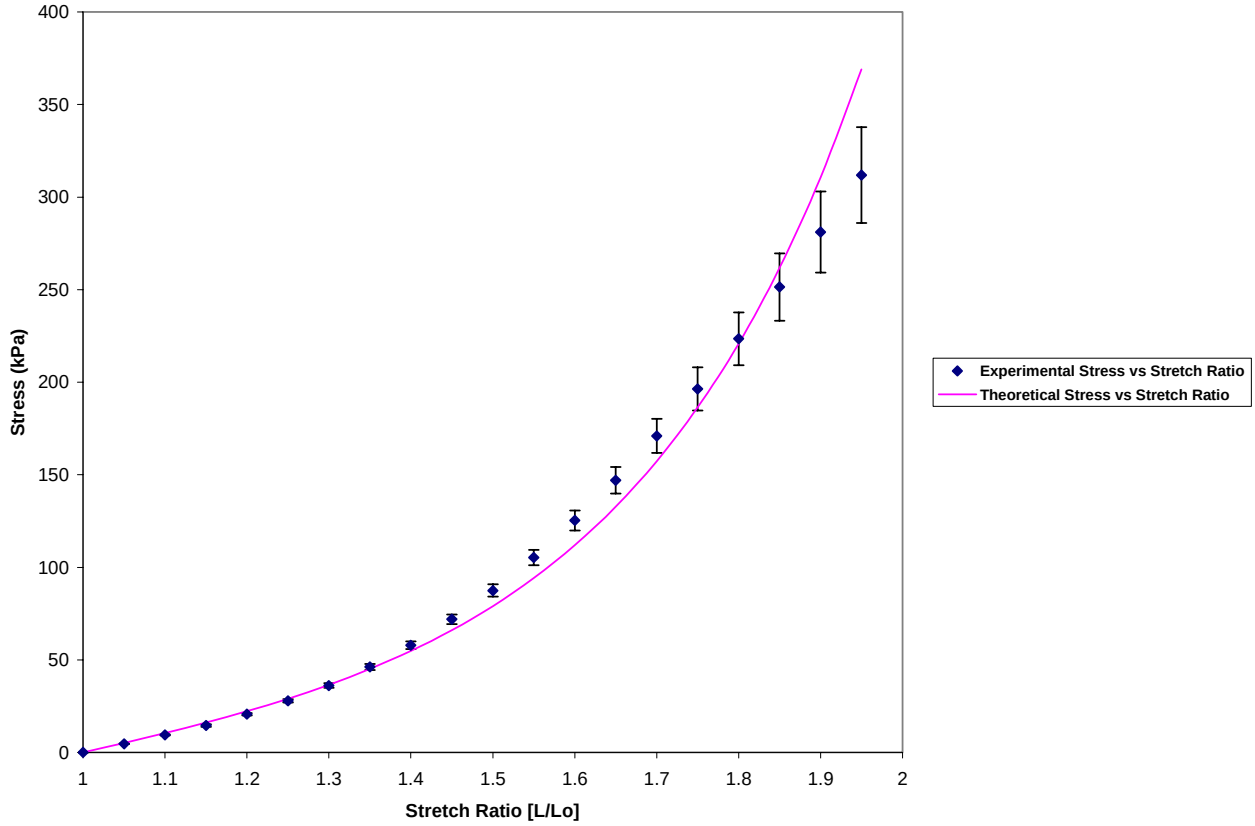

Figure 8c: Theoretical and experimental 1D response of a strip (10%, 6 cycle PVA hydrogel)

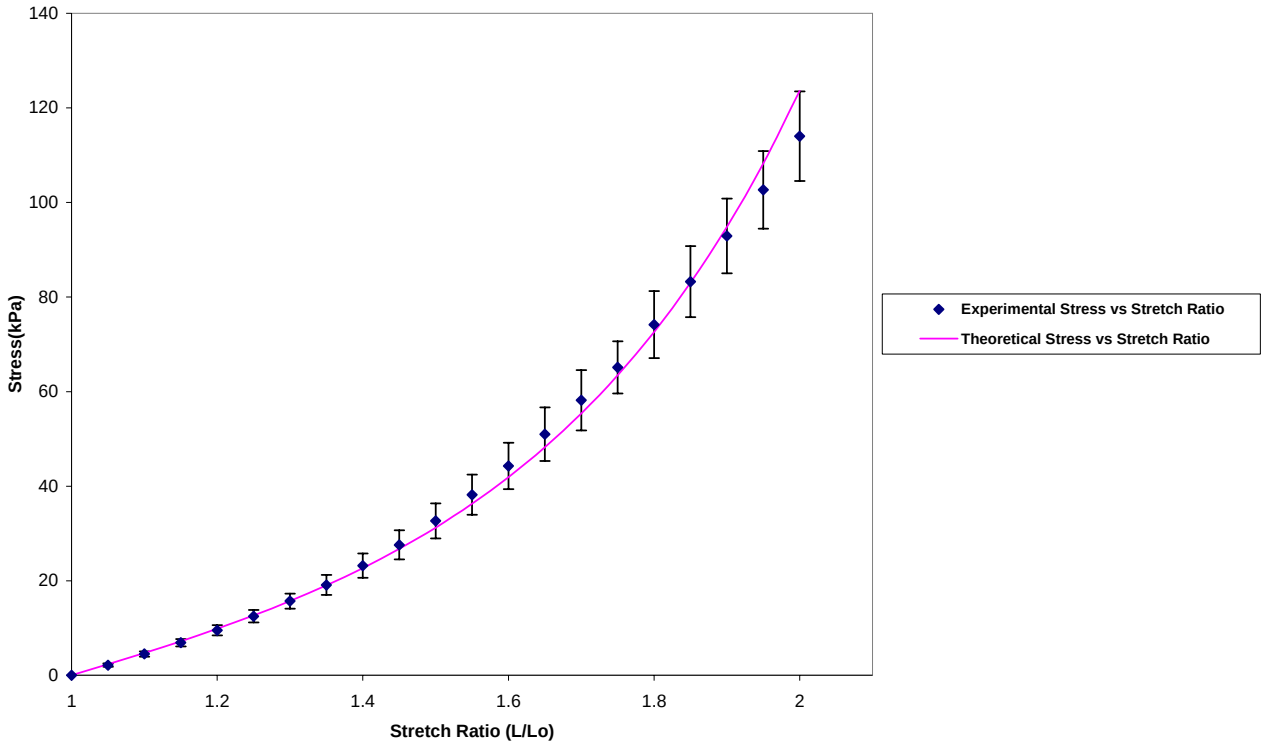

Figure 8d: Theoretical and experimental 1D response of a strip (15%, 2 cycle PVA hydrogel)

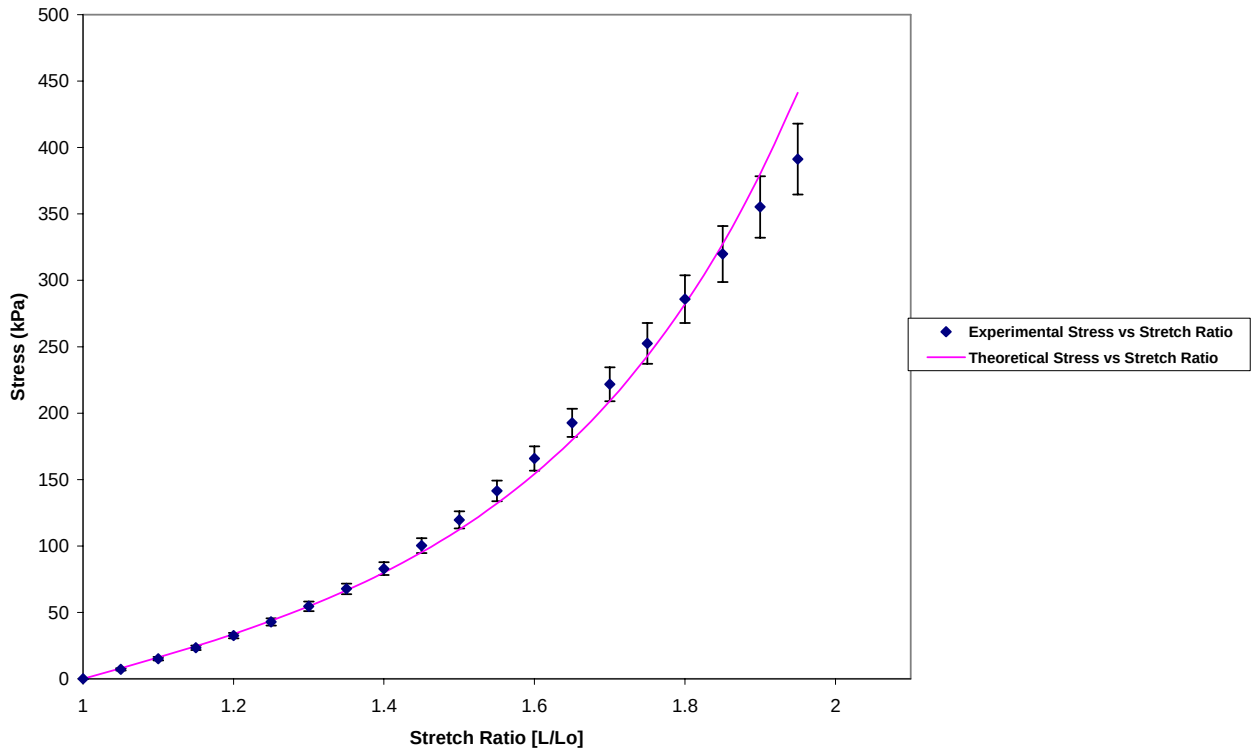

Figure 8e: Theoretical and experimental 1D response of a strip (15%, 4 cycle PVA hydrogel)

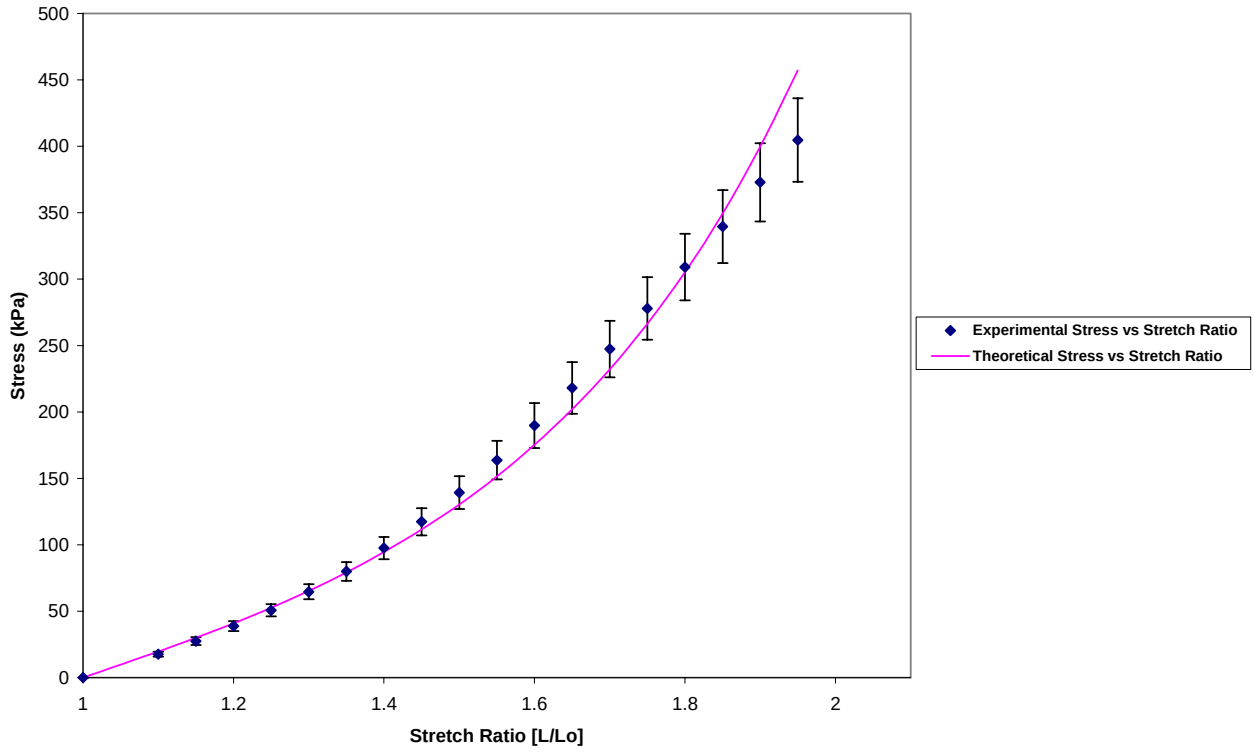

Figure 8f: Theoretical and experimental 1D response of a strip (15%, 6 cycle PVA hydrogel)

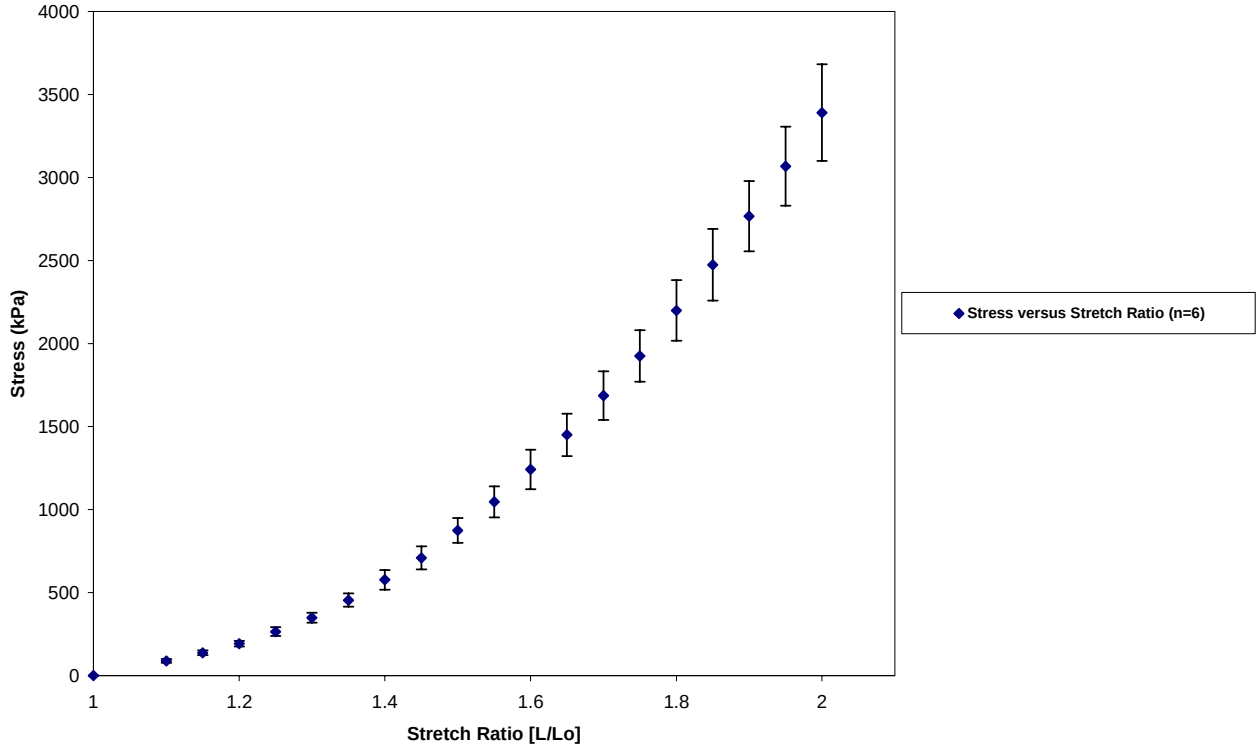

Figure 9: Average experimental stress versus stretch ratio of a ring (Salubria-TM biomaterial)

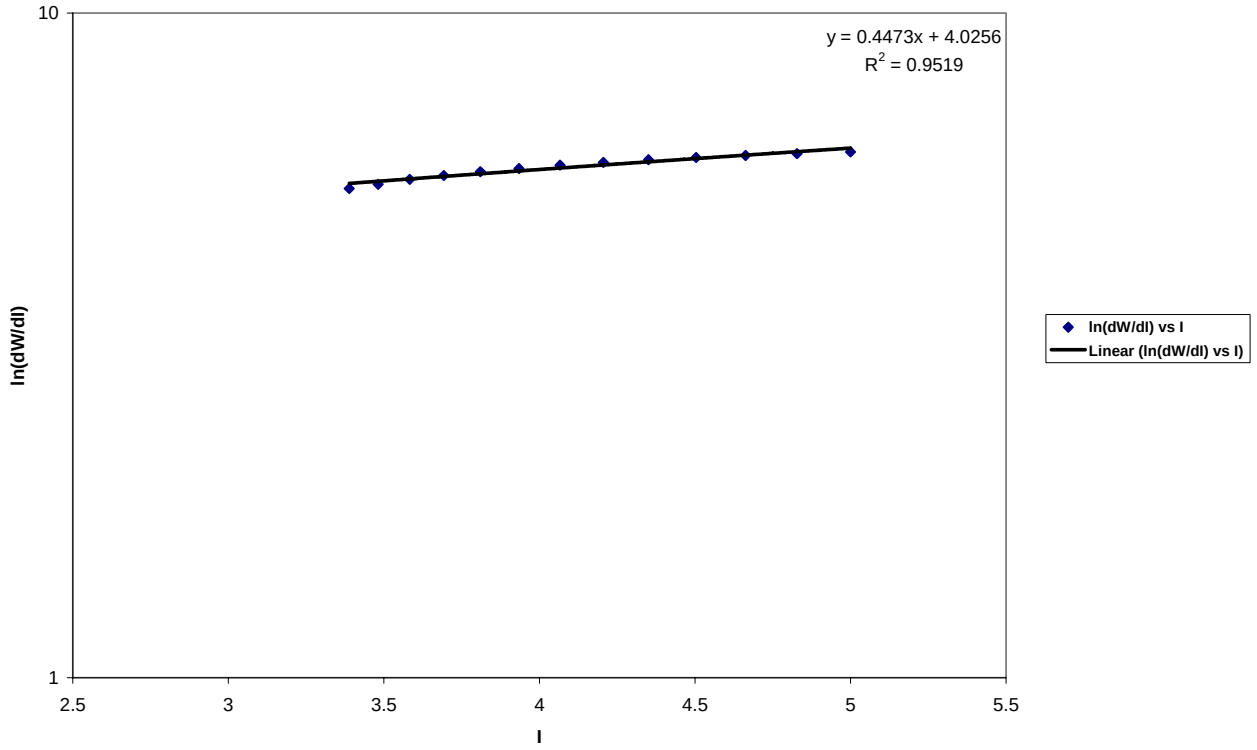

Figure 10: Average experimental ln(dW/dI) versus I of a ring (Salubria-TM biomaterial)

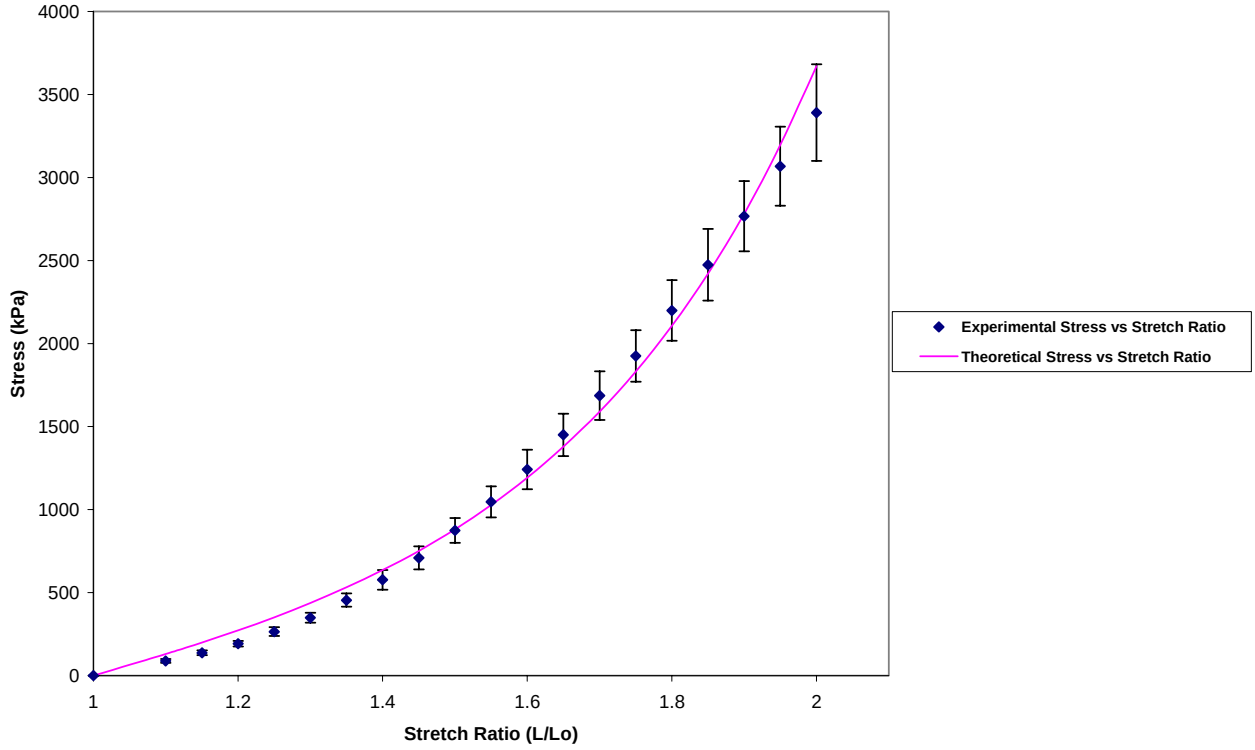

Figure 11: Theoretical and experimental 1D response of a ring (Salubria-TM biomaterial)

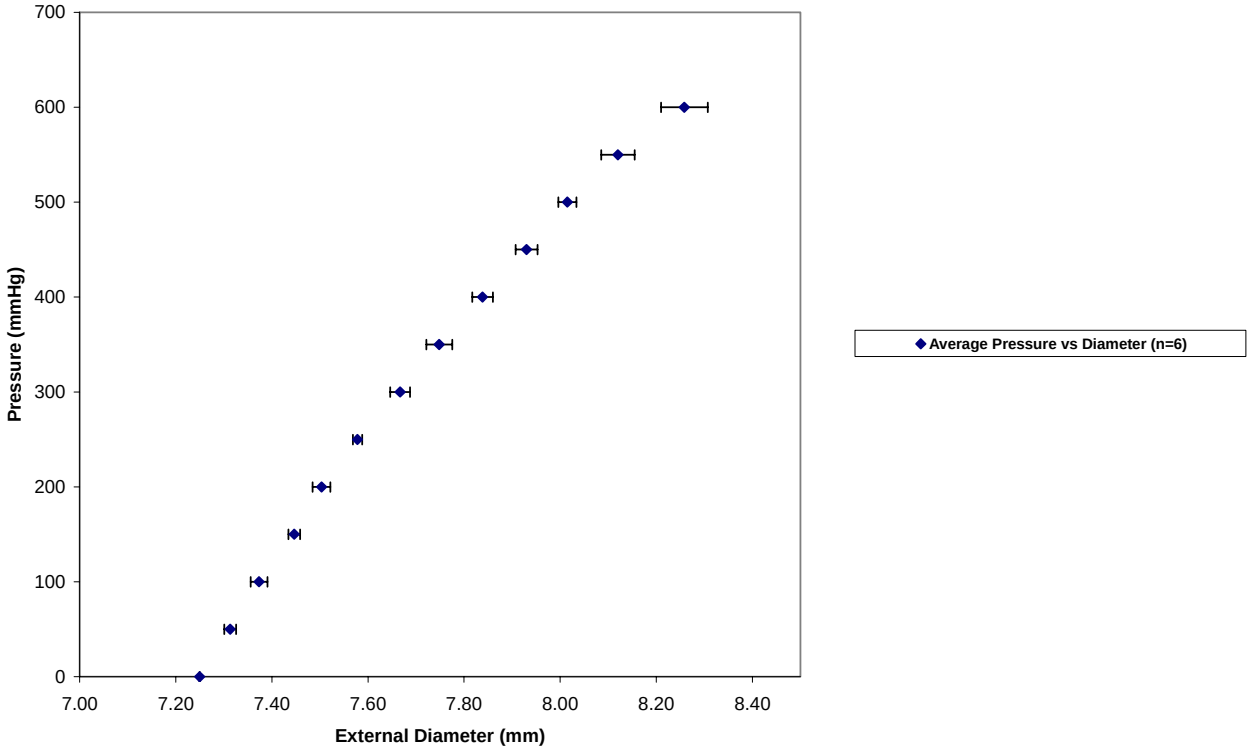

Figure 12a: Experimental 3D response of tube 1 (Salubria-TM biomaterial)

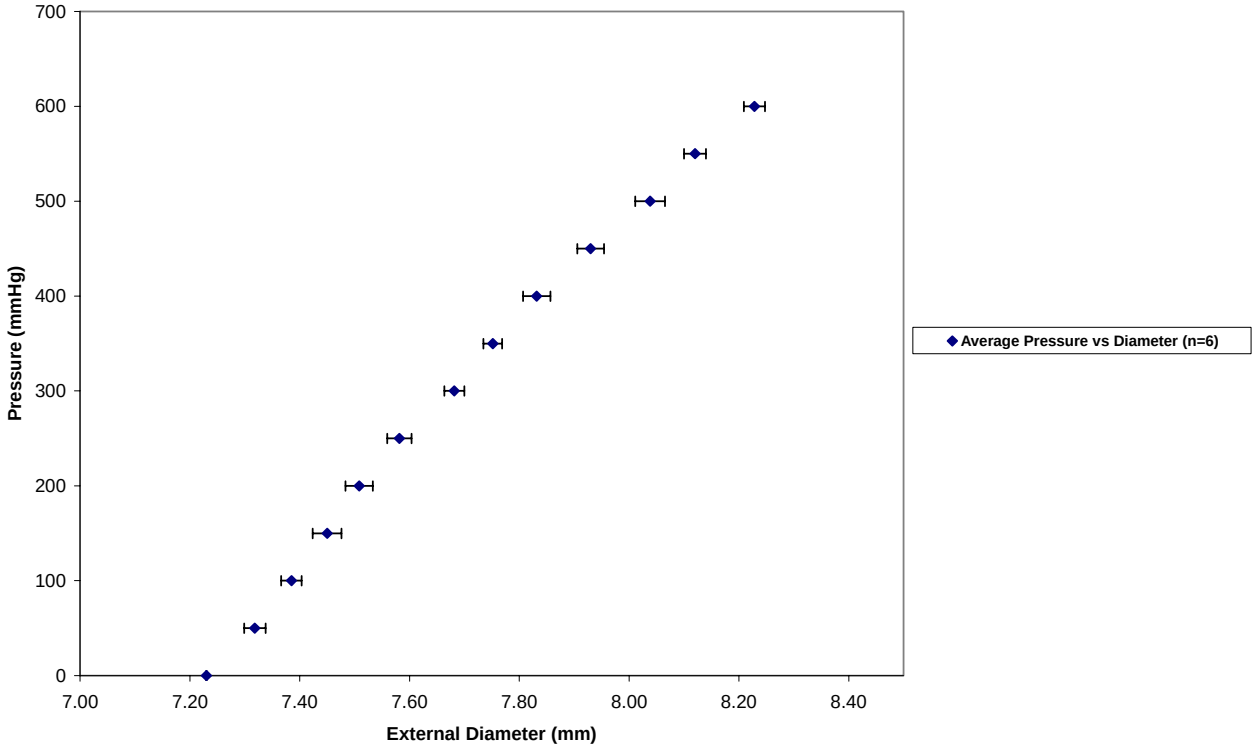

Figure 12b: Experimental 3D response of tube 2 (Salubria-TM biomaterial)

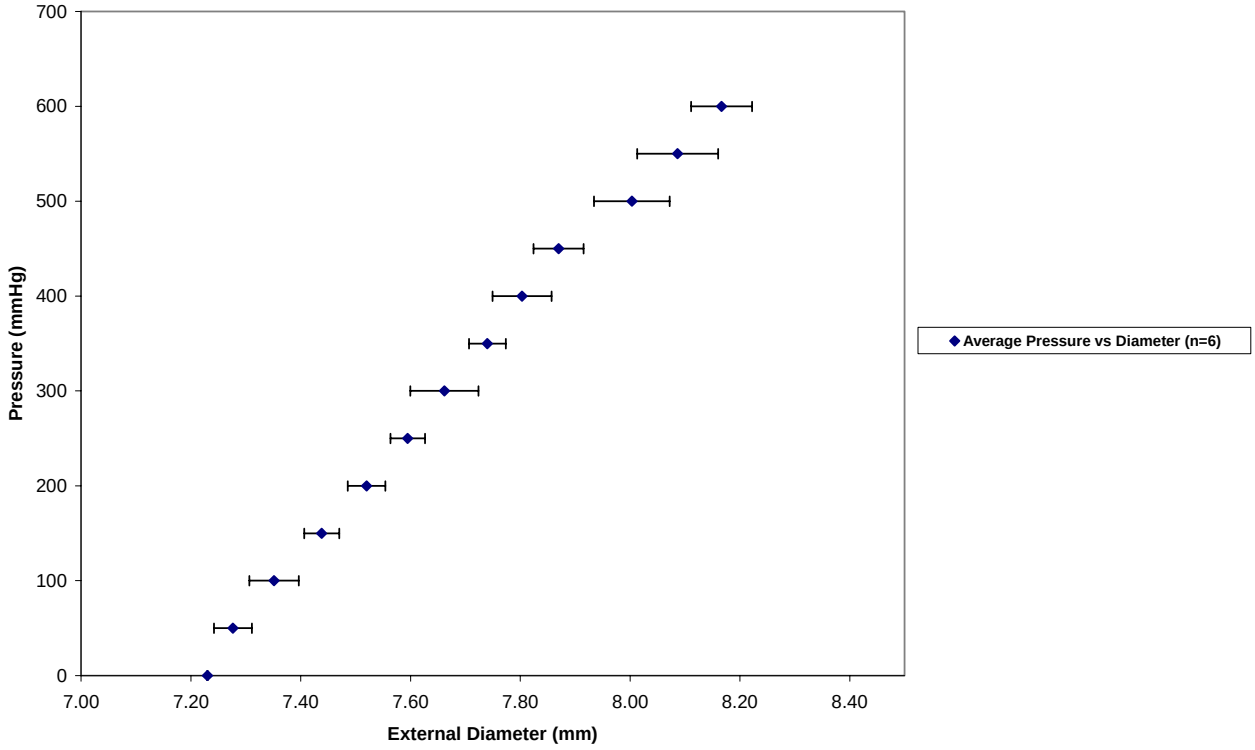

Figure 12c: Experimental 3D response of tube 3 (Salubria-TM biomaterial)

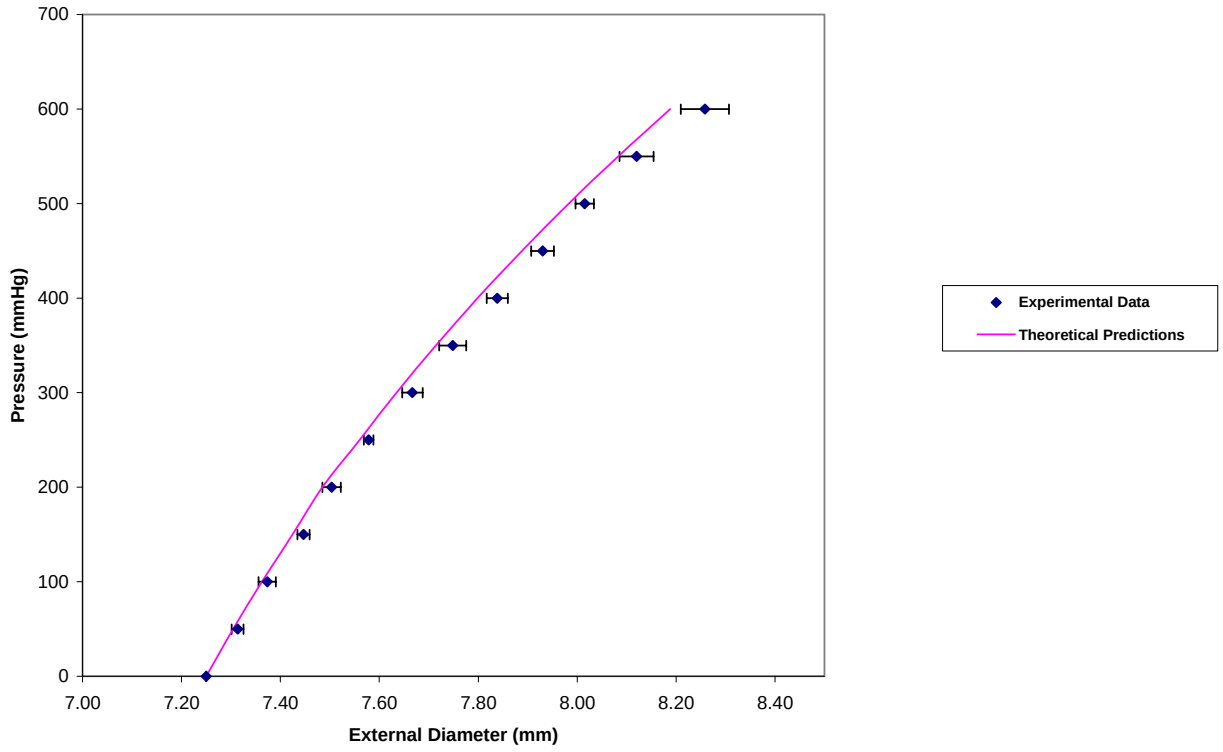

Figure 13a: Theoretical and experimental 3D response of tube 1 (Salubria-TM biomaterial)

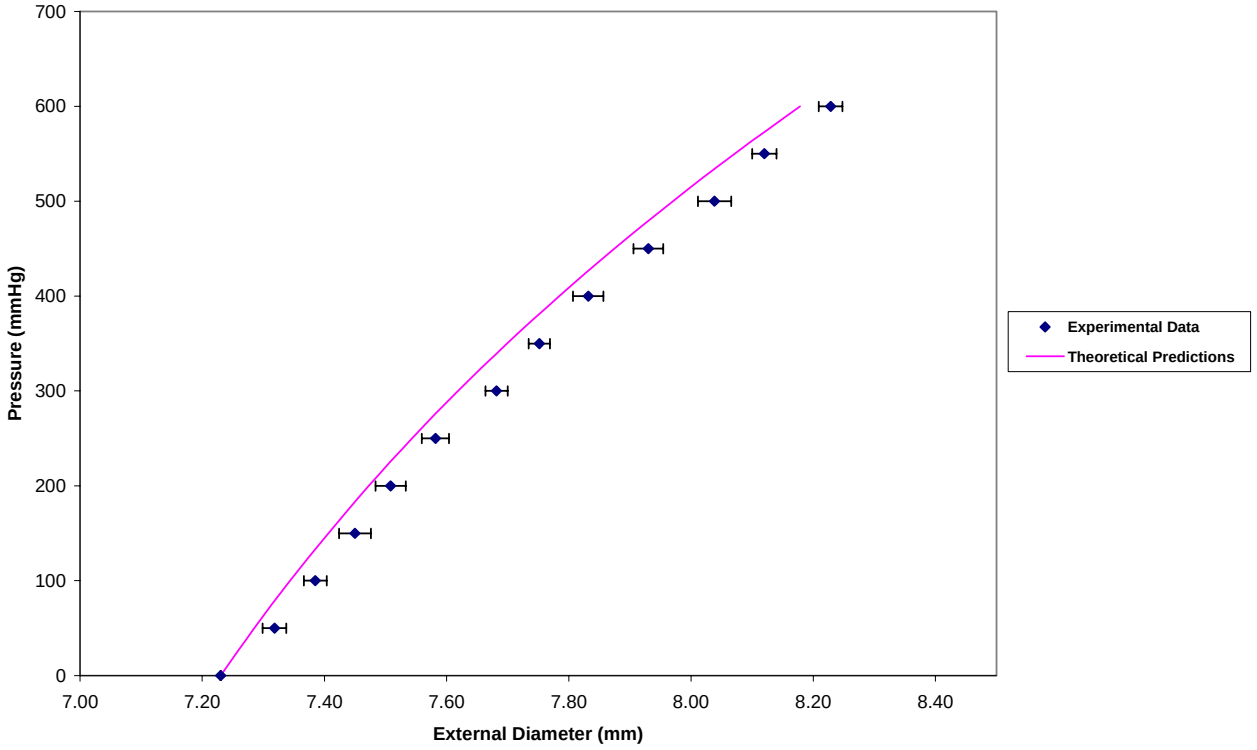

Figure 13b: Theoretical and experimental 3D response of tube 2 (Salubria-TM biomaterial)

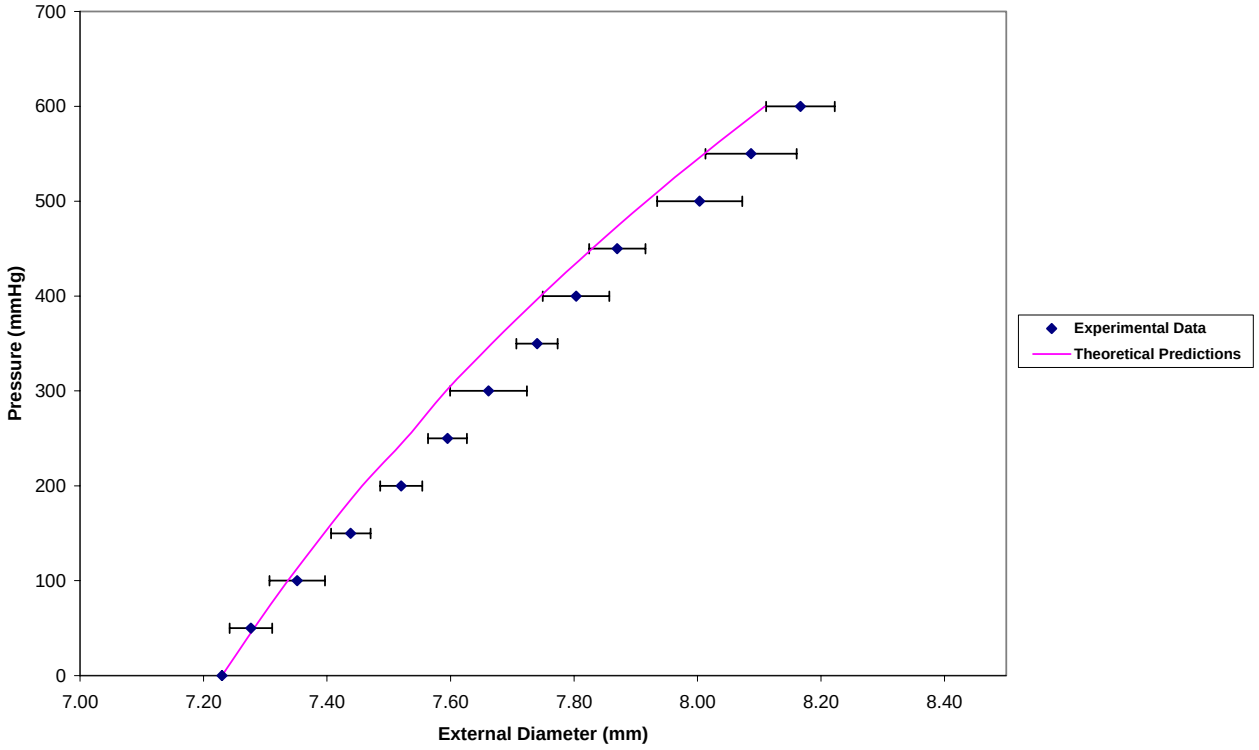

Figure 13c: Theoretical and experimental 3D response of tube 3 (Salubria-TM biomaterial)

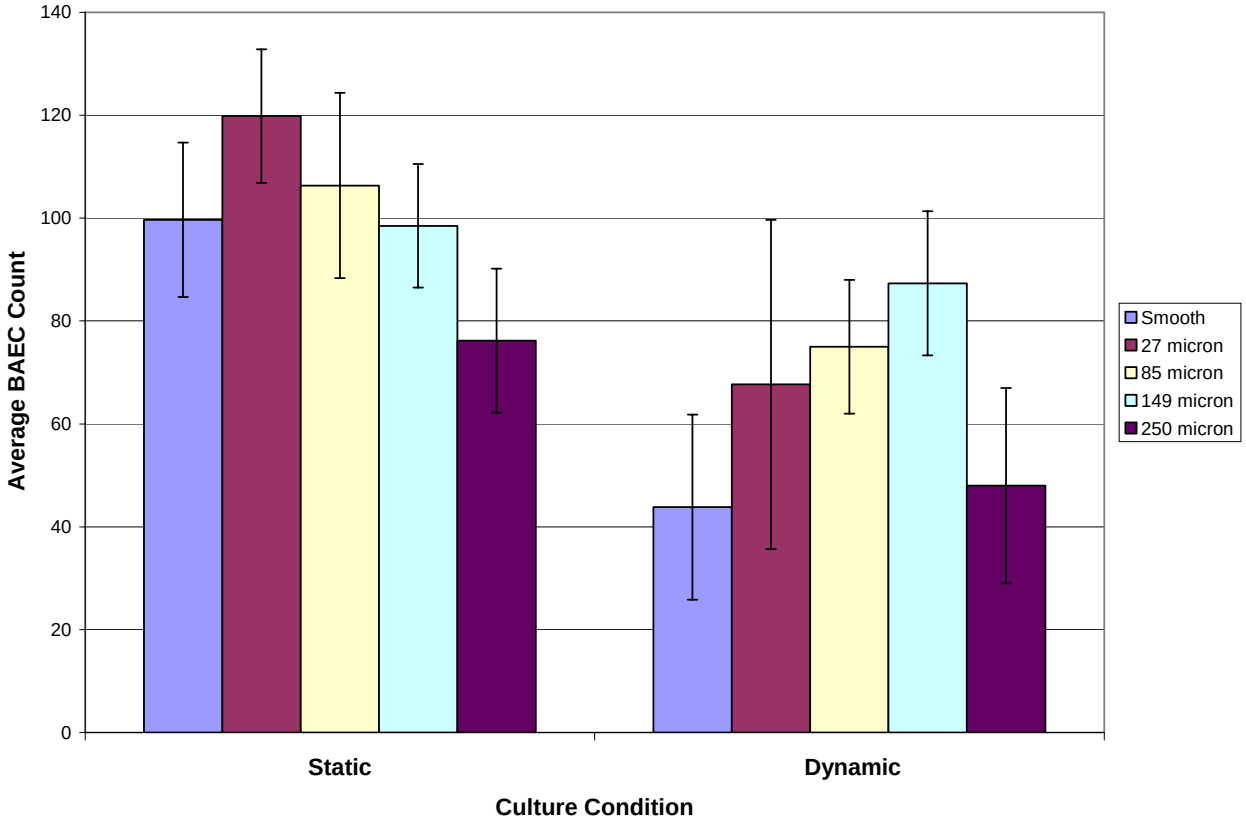

Figure 14: BAEC count versus PVA surface roughness for static and dynamic culture conditions

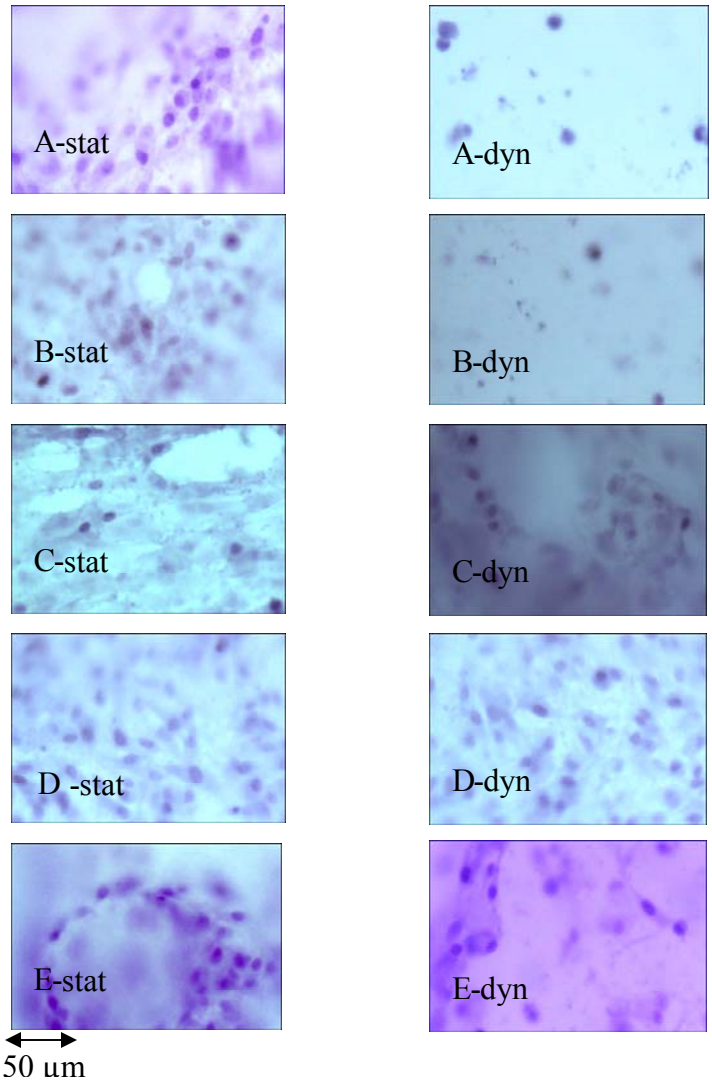

Figure 15: PVA specimen counterparts for static and dynamic culture conditions (A - smooth, B - 27µm roughness, C - 85µm roughness, D - 149µm roughness, E - 250µm roughness)

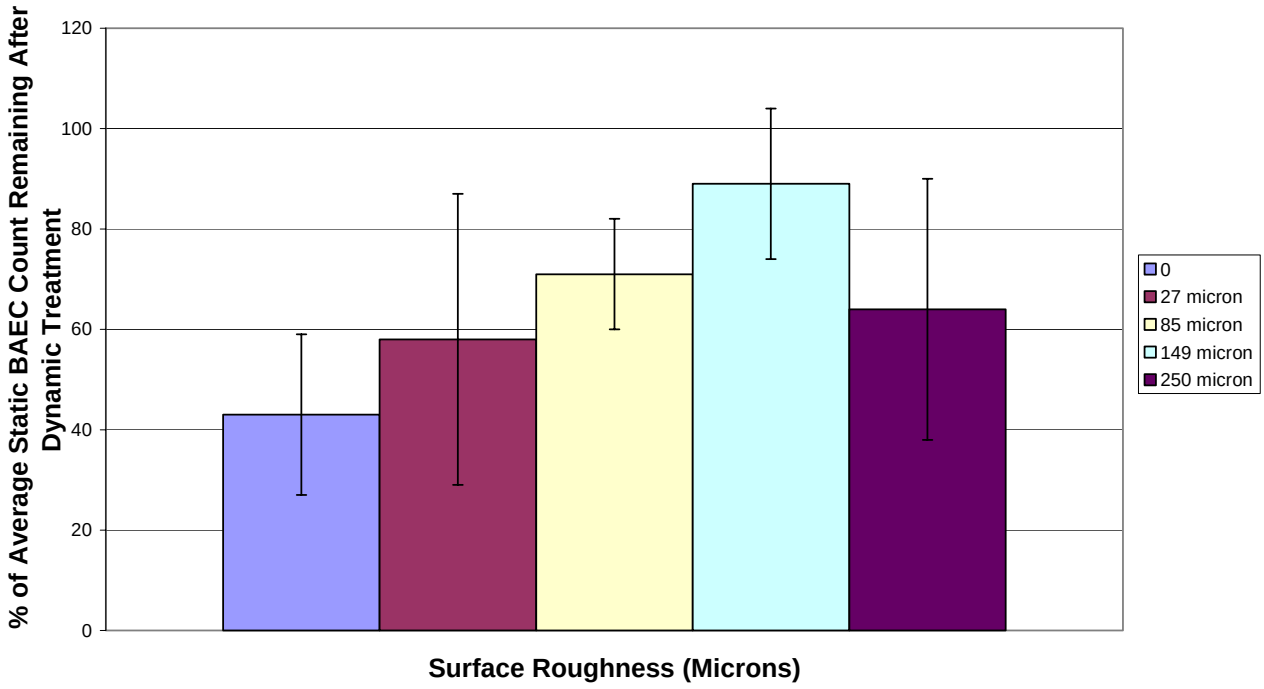

Figure 16: Average % of static treatment BAEC count remaining after dynamic treatment for related specimens

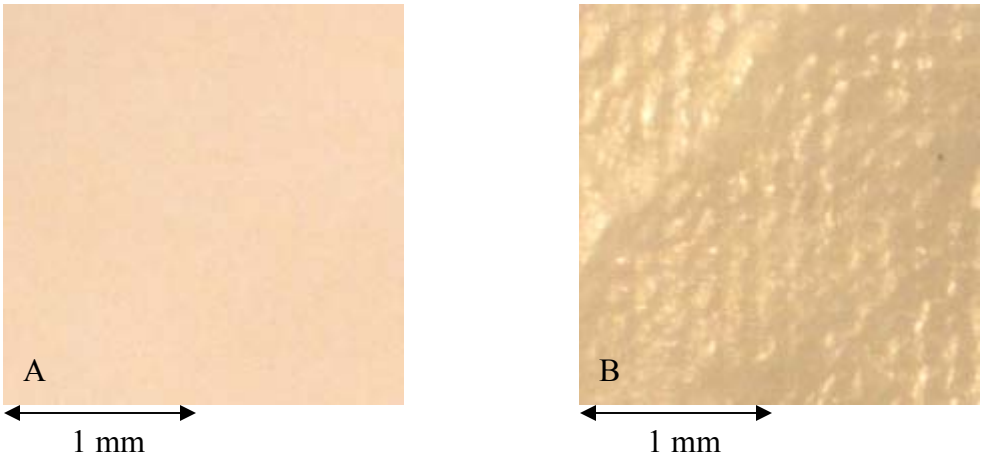

Figure 17: PVA hydrogels with (A) smooth surface and (B) 149-micron surface roughness pattern

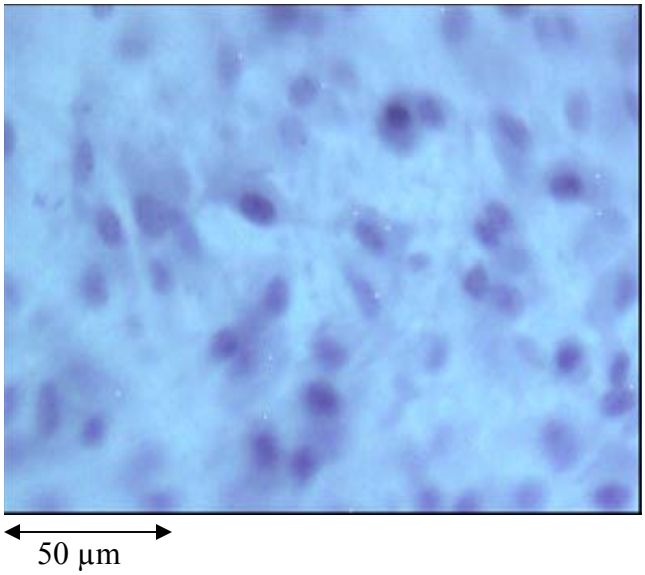

Figure 18a: Example of morphological assessment of adhesive BAEC (1 rating – highest rating for adhesion)

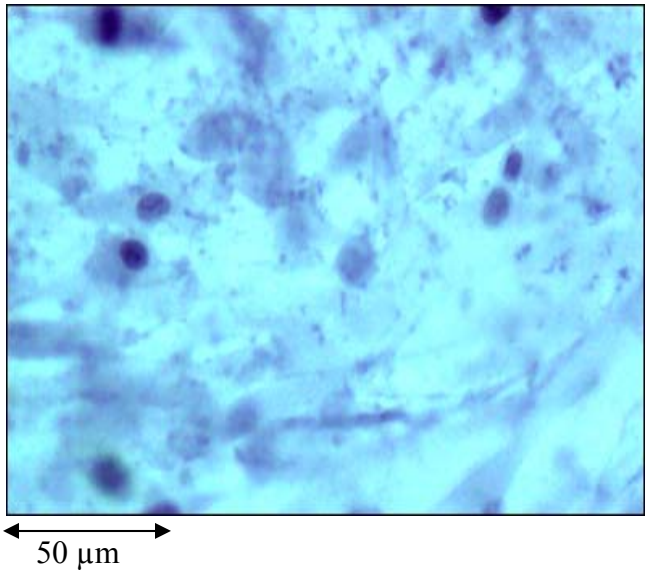

Figure 18b: Example of morphological assessment of adhesive BAEC (2 rating – mediocre rating for adhesion)

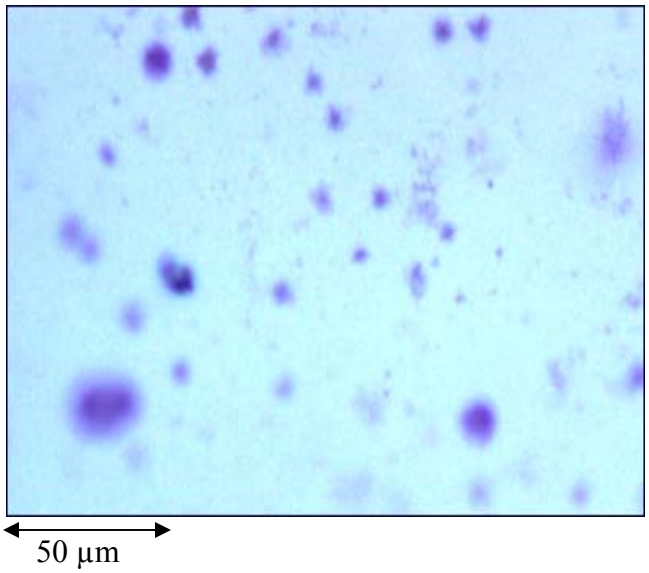

Figure 18c: Example of morphological assessment of adhesive BAEC (3 rating – lowest rating for adhesion)

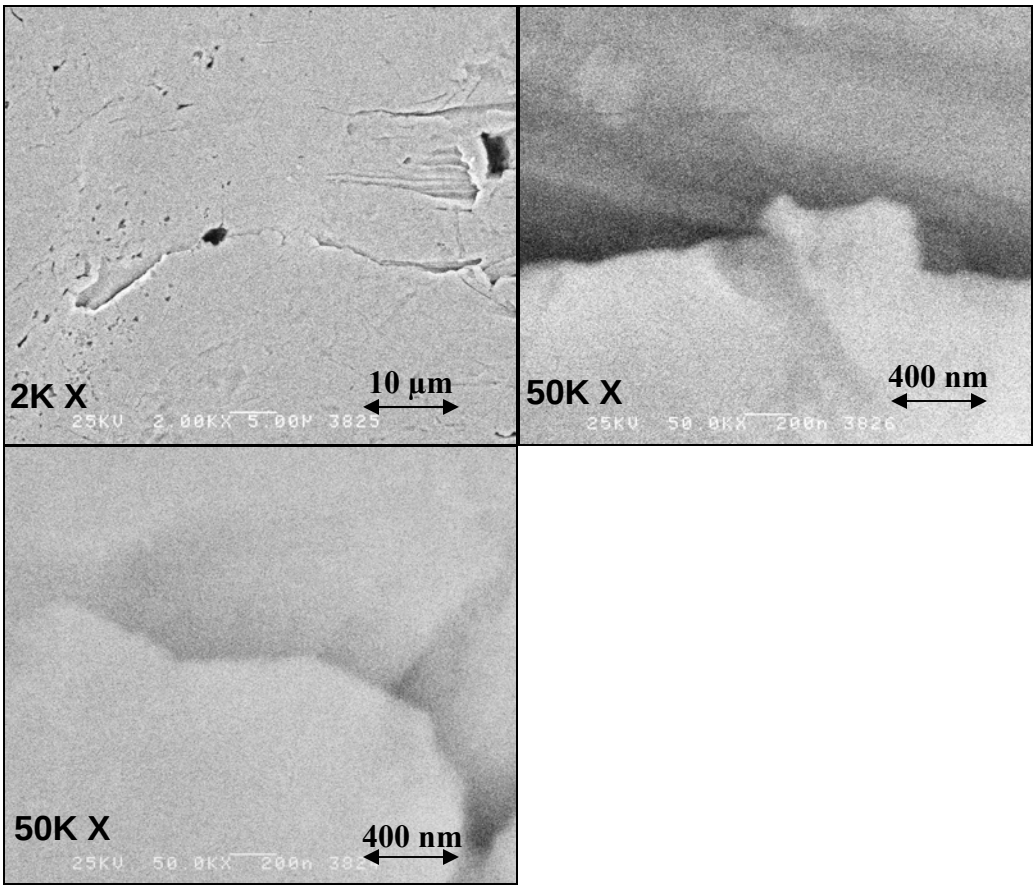

Figure 19a: cHRSEM images of Sample A (5 minute etch time, magnification X indicated on each image)

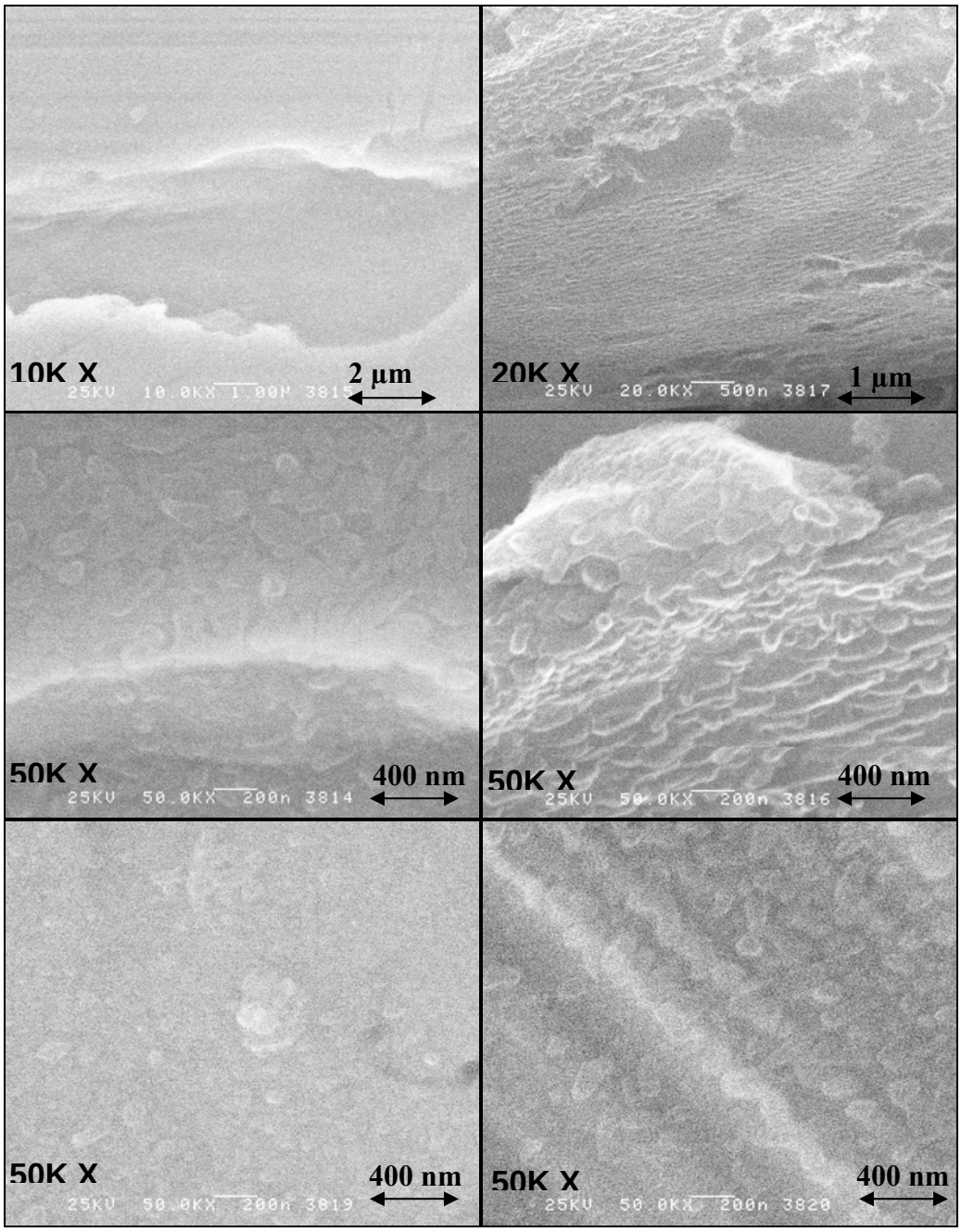

Figure 19b: cHRSEM images of Sample A (3 minute etch time, magnification X indicated on each image)

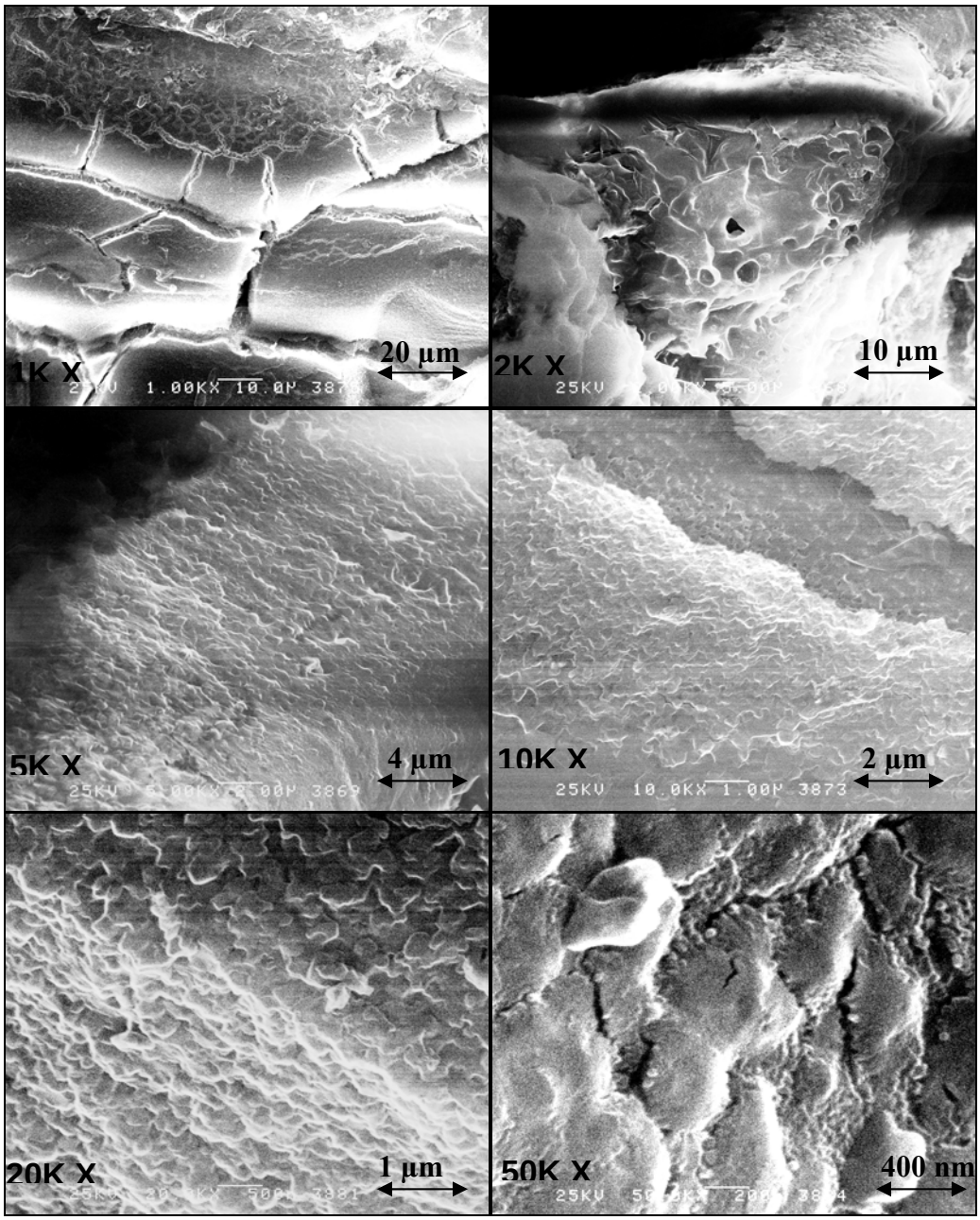

Figure 19c: cHRSEM images of Sample B (No etching, magnification X indicated on each image)

REFERENCES

1. Davids L, Dower T, Zilla, P. The lack of healing in conventional vascular grafts. Tissue Engineering of Prosthetic Vascular Grafts. Zilla and Greisler, 1999. RG Landes Co.

2. Kadar KN, Sweany JM, Bellamkonda RV. Cationic lipid-mediated transfecion of bovine aortic endothelial cells inhibits their attachment. J of Biomed Mater Res 2002; 60: 405-410.

3. Nerem RM, Seliktar D. Vascular tissue engineering. Annu. Rev. Biomed. Eng. 2001; 3: 225-243.

4. Salam TA, Lumsden AB, Suggs WD, Ku DN. Low shear stress promotes intimal hyperplasia thickening. Journal of Vascular Investigation 1996; 2(1): 12-22.

5. Seifalian AM, Giudiceandrea A, Schmitz-Rixen T, Hamilton G. Noncompliance: The silent acceptance of a villain. Tissue Engineering of Prosthetic Vascular Grafts. Zilla and Greisler 1999. RG Landes Co.

6. Peppas NA, Lustig SR. Solute diffusion in hydrophilic network structures. Hydrogels in medicine and pharmacy 1986; 1: 57-84.

7. Amsden B. Solute diffusion within hydrogels: mechanism and models. Macromolecules 1998; 31: 8382-8395.

8. Jarrell BE, Williams SK, Stokes G. Use of freshly isolated capillary endothelial cells for the immediate establishment of a monolayer on a vascular graft at surgery. Surgery 1986; 100: 392-399.

9. Schmidt SP, Hunter TJ Sharp WV. Endothelial cell seeded four-millimeter Dacron vascular grafts. J. Vas. Surg 1984; 1: 434-441.

10. Mazzucotelli JP, Moczar M, Zede L Bambang LS, Loisance D. Human vascular endothelial cells on ePTFE precoated with engineered protein adhesion factor. Int. J. Artif. Org. 1994; 17: 112-117.

11. Hern DL, Hubbell JA. Incorporation of adhesion peptide into nonadhesive hydrogels useful for tissue resurfacing. J. of Biomed. Mater. Res 1998; 39: 266-276.

12. Greisler HP, Gosselin C, Ren D, Kang SS, Kim DU. Biointeractive polymers and tissue engineered blood vessels. Biomaterials 1996; 17: 329-336.

13. Fields C, Cassano A, Makhoul RG. Evaluation of electrostatically endothelial cell seeded expanded PTFE grafts in a canine femoral artery model. Journal of Biomaterials Applications 2002; Vol 17: 135-150.

14. Clagett GP, Burkel WE, Sharefkin JB. Plate let activity in dogs with arterial prosthesis seeded with endothelial cells. Circulation 1984; 69: 632-639.

15. Kempczinski RF, Ramalanjaona GR, Douville C, Silberstein EB. Thrombogenicity of a fibronectin-coated, experimental polytetrafluoroethylene graft. Surgery 1987; 101: 439-444.

16. Clowes AW, Reidy MA. Mechanisms of arterial graft failure: the role of cellular proliferation. Ann. N.Y. Acad. Sci. 1987; 516: 673-678.

17. Clowes AW, Gown AM, Hanson SR, Reidy MA. Mechanisms of arterial graft failure: the role of cellular proliferation in early healing of PTFE prosthesis. Ann J Pathology 1985; 118(1): 43-54.

18. Golden MA, Hanson SR, Kirkman TR, Schneider PA, Clowes AW. Mechanisms of arterial graft failure II: chronic endothelial and smooth muscle cell proliferation in healing polytetrafluoroethylene prostheses. J Vasc Surg. 1986; 11(6): 877-884.

19. Wu MH, Shi Q, Wecheak AR, Clowes AW, Gordon IL, Sauvagae LR. Definitive proof of endothelialization of a Dacron arterial prosthesis in a human being. J of Vasc. Surgery 1995; 21: 862-867.

20. Shi Q, Hong M, Onuki Y, Ghali R, Hunter GC, Johansen KH, Sauvagae LR. Endothelium on the flow surface of human aortic Dacron vascular grafts. J of Vasc. Surgery 1997; 25: 737-742.

21. Berger K, Sauvagae LR, Rao AM, Wood SJ. Healing of arterial prosthesis in man: Its incompleteness. Ann. Surg. 1972; 175: 118-127.

22. Wesolowski SA, Fries CC, Gennigar G, Fox LM, Sawyer PN, Sauvagae LR. Factors contributing to the long term failure of human vascular prosthetic grafts. Cardiovasc. Surg. 1964; 38: 544-567.

23. Sauvagae LR, Berger K, Wood SJ, Nakagawa Y, Mansfield PB. An external velour surface for porous arterial prosthesis. Surgery 1971; 70: 940-953.

24. Sauvagae LR, Berger K, Mansfield PB. Future directions in the development of arterial prosthesis for small and medium caliber arteries. Surgery 1974; 54: 213-228.

25. Clagette PC. In vivo evaluation of platelet activity with vascular prosthesis. In: Stanley JC, ed. Biologic and Synthetic Vascular Prosthesis. New York: Grune and Stratton 1982: 131-152.

26. Zamora JL, Navarro LT, Ives CL, Weilbaecher DG, Gao ZR, Noon GP. Seeding of arteriovenous prosthesis with homologous endothelium. J Vasc Surg 1986; 3: 860-866.

27. Graham LM, Burkel WE, Ford WJ, Vinter DW, Kahn RH, Stanley JC. ePTFE vascular prosthesis seeded with enzymatically derived and cultured canine endothelial cells. Surgery 1982; 91: 550-559.

28. Harrison HJ. Synthetic materials as vascular prosthesis. A comparative study in small vessels of nylon, dacron, orlon, ivalon, and teflon. Amer J of Surg 1958; 95: 3-15.

29. Wesolowski SA, Fries CC, Karlson KE, De Bakely M, Sawyer PN. Porosity: Primary determinant of ultimate fate of synthetic vascular grafts. Surgery 1961; 50: 90-96.

30. Golden MA, Hanson SR, Kirkman TR, Schneider PA, Clowes AW. Healing of polytetrafluoroethylene arterial grafts is influenced by graft porosity. J Vasc Surg. 1990; 11(6): 838-844.

31. Clowes AW, Kirkman TR, Clowes MM. Mechanisms of arterial graft failure II. Chronic endothelial and smooth muscle cell proliferation in healing of PTFE prosthesis. J Vasc Surg. 1986; 3: 877-884.

32. Clowes AW, Zacharias RK, Kirkman TR, Early endothelial coverage of synthetic arterial grafts: porosity revisited. The Amer J Surg 1987; 153: 501-504.

33. Kumar TR, Krishnan LK. A stable matrix for generation of tissue-engineered nonthrombogenic vascular grafts. Tissue Engineering 2002; 8(5): 763-769.

34. Ratcliff A. Tissue engineering of vascular grafts. Matrix Biology 2000; 19, 353-357.

35. Fields C, Cassano A, Bowlin GL. Endothelial cell seeding of a 4-mm i.d. polyurethane vascular graft. Journal of Biomaterials Applications 2002; 17: 45-68.

36. Schneider PA, Hanson SR, Price TM, Harker LA. Preformed confluent endothelial cell monolayers prevent early platelet deposition on vascular prosthesis in baboons. J. Vasc. Surg. 1988; 8: 229-235.

37. Herring MB, Baughman S, Glover J. Endothelial seeding of Dacron and polytetrafluoroethylene grafts: The cellular events of healing. Surgery 1984; 96: 745-754.

38. Zhang H, Williams GM. Capillary and venule proliferation in the healing process of Dacron venous grafts in rats. Surgery 1992; 111: 409-415.

39. Merzkirch C, Davies N, Zilla P. Engineering of vascular ingrowth matrices: Are protein domains an alternative to peptides? The Anatomical Record 2001; 263: 379-387.

40. Baird RN, Abbot WM. Pulsatile blood-flow in arterial grafts. The Lancet 1976; 30: 948-949.

41. Abbott WM, Mergerman JM, Hasson JE. Effect of compliance mismatch upon vascular graft patency. J of Vasc Surg 1987; 5: 376-382.

42. SaluMedica, Atlanta. Salubria-TM biomaterial.

43. Apkarian RP, Wright ER, Seredyuk VA, Eustis S, Lyon LA, Conticello VP, Menger FM. In-lens cryo-high resolution scanning electron microscopy: Methodologies for molecular imaging of self-assembled organic hydrogels. Microscopy and Microanalysis 2003; 9: 1-10.

44. Wright ER, Conticello VP, Apkarian RP. Morphological characterization of elastin-mimetic block copolymers utilizing cryo- and cryoetch-HRSEM. Microscopy and Microanalysis 2003; 9: 1-12.

45. Delfino A, Stergiopulos N, Moore JE, Meister JJ. Residual stain effects on the stress field in a thick walled finite element model of the human carotid bifurcation. J of Biomechanics 1997; 30: 777-786.

46. Rachev, A. Lecture notes on selected topics of the theory of finite deformation given in the laboratory of Dr. David Ku. 2003.

47. Kawasaki T, Sasayama S, Yagi S, Asakawa T, Hirai T. Non-invasive assessment of the age-related changes in stiffness of major branches of the human arteries. Cardiovasc Res 1987; 21: 678-687.

48. Castillo EJ, Koeing JL, Anderson JM, Lo J. Protein absorption on hydrogels. Biomaterials 1985; 6: 338-345.

49. van Wachem FB, Beugeling T, Feijen J, Bantjies A, Detmers JP, van Aken WG. Interaction of cultured human endothelial cells with polymeric surfaces of different wettabilities. Biomaterials 1985; 6: 403-408.